Theoretical Study of the Isomerization Mechanism of Azobenzene and Disubstituted Azobenzene Derivatives

Christina R. Crecca and Adrian E. Roitberg*

Department of Chemistry and Quantum Theory Project, University of Florida, Gainesville, Florida 32611

Received: December 20, 2005; In Final Form: May 7, 2006

A series of azobenzenes was studied using ab initio methods to determine the substituent effects on the isomerization pathways. Energy barriers were determined from three-dimensional potential energy surfaces of the ground and electronically excited states. In the ground state (S_0), the inversion pathway was found to be preferred. Our results show that electron donating substituents increase the isomerization barrier along the inversion pathway, whereas electron withdrawing substituents decrease it. The inversion pathway of the first excited state (S_1) showed trans → cis barriers with no curve crossing between S_0 and S_1. In contrast, a conical intersection was found between the ground and first excited states along the rotation pathway for each of the azobenzenes studied. No barriers were found in this pathway, and we therefore postulate that after n → π^* ($S_1 \leftarrow S_0$) excitation, the rotation mechanism dominates. Upon $\pi \rightarrow \pi^*$ ($S_2 \leftarrow S_0$) excitation, there may be sufficient energy to open an additional pathway (concerted-inversion) as proposed by Diau. Our potential energy surface explains the experimentally observed difference in trans-to-cis quantum yields between S_1 and S_2 excitations. The concerted inversion channel is not available to the remaining azobenzenes, and so they must employ the rotation pathway for both n → π^* and $\pi \rightarrow \pi^*$ excitations.

I. Introduction

Azobenzene can adopt cis and trans conformations in the electronic ground state with the trans isomer lower in energy by approximately 0.6 eV[1]. The trans to cis energy barrier was found experimentally to be about 1.6 eV[2]. Azobenzene is known to undergo a reversible photoisomerization between these conformations. A trans to cis isomerization occurs upon excitation at 365 nm (3.40 eV) and a cis to trans isomerization takes place at 420 nm (2.95 eV).[3] A thermally induced cis to trans isomerization is also possible in the ground state. Because of their facile interconversion at appropriate wavelengths, azobenzenes have the potential to be used in optical switching and image storage devices[4−7] as well as molecular scissors[8] and as targets for coherent control in molecular electronics.[9]

There are two pathways by which isomerization is thought to take place. The rotation pathway occurs by an out of plane torsion of the CNNC dihedral angle labeled ϕ in Figure 1. The inversion pathway involves an in-plane inversion of the NNC angle between the azo group and the adjacent carbon of the benzene ring. The inversion angle is labeled φ in Figure 1. An interesting and somewhat puzzling aspect of the photochemistry of azobenzenes is the difference in trans to cis quantum yield upon excitation to the dark $S_1(n\pi^*)$ state ($\Phi = 0.20$[3,10]-0.36[11]) and bright $S_2(\pi\pi^*)$ state ($\Phi = 0.09$[3,10]-0.20[11]). Even within this large experimental range $\Phi(S_1)$ is clearly larger than $\Phi(S_2)$. When the rotation pathway is blocked by restricting the NN bond rotation with a crown ether,[12] cyclophane structure,[13] or within a cyclodextrin cavity,[14] the difference in quantum yield disappears. This observation led to the belief that isomerization occurs by different mechanisms after the n → π^* and $\pi \rightarrow \pi^*$ excitations.

Most researchers agree that the inversion mechanism dominates in the ground state,[15,21,30,39] but until recently there was much debate over which mechanism dominates after excitation to each excited state. Monti's[15] minimal basis set CI calculations provided the first theoretical explanation: excitation to S_1 resulted in isomerization via the inversion pathway while the rotation pathway dominated after S_2 excitation. His potential energy curves were adopted by most experimentalists and used to explain their results.

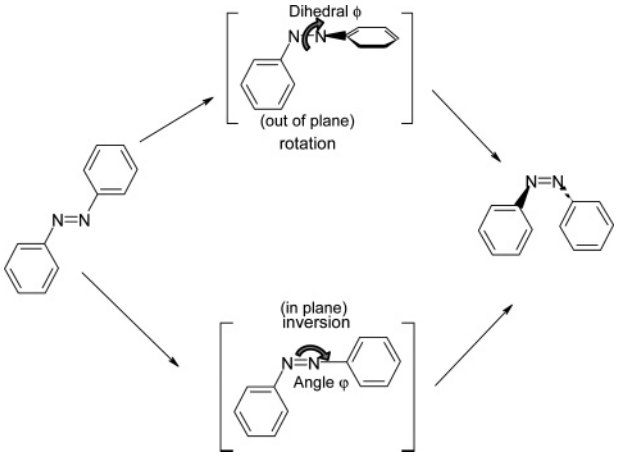

Figure 1. Schematic diagram of the rotation and inversion pathways of the trans → cis isomerization of azobenzenes. The rotation pathway is obtained by a torsion of the azo group around the CNNC dihedral angle ϕ. The inversion pathway is obtained by an in-plane inversion of the NNC angle (angle φ) formed between the azo group and the attached carbon of one of the benzene rings.

Time-resolved UV−visible absorption spectroscopy of azobenzene by Lednev shows that upon excitation of *trans*-azobenzene at $\lambda_{exc} = 280-347$ nm, two transients are formed.[16−18] One was determined to be fast decaying, 1 ps, corresponding to the S_2 state and the other was longer-lived, 10−16 ps, corresponding

* To whom correspondence should be addressed. E-mail: roitberg@ufl.edu

10.1021/jp057413c CCC: $33.50
Published on Web 06/15/2006

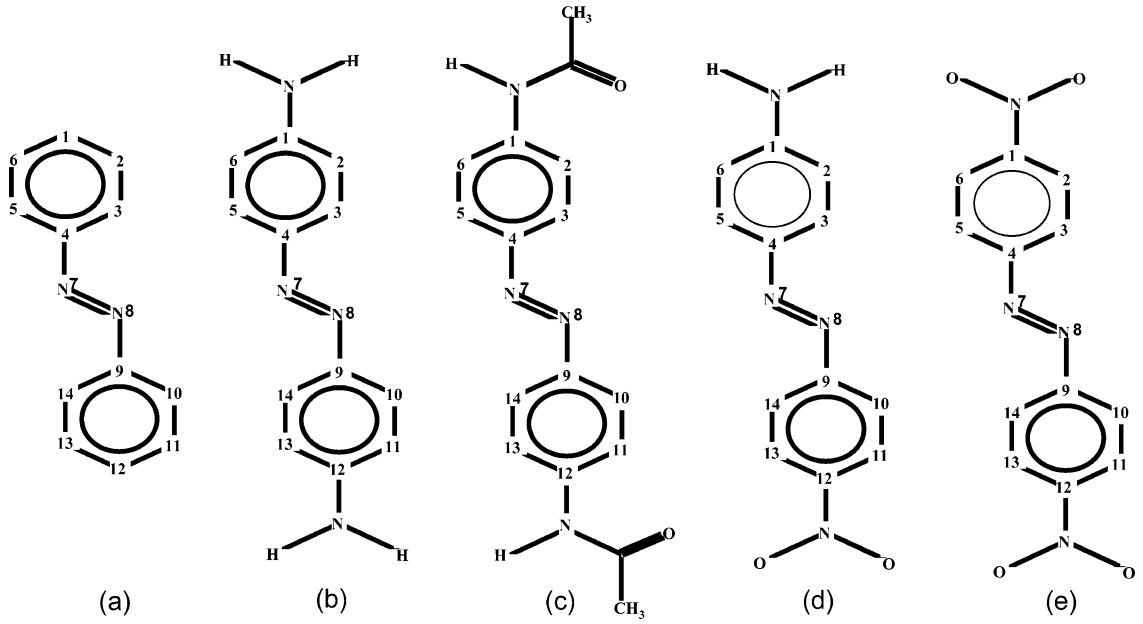

Figure 2. Structures of compounds investigated in this work: (a) Azo, (b) Azon, (c) Azonco, (d) $AzoNO_2NH_2$, and (e) $AzoNO_2NO_2$. This numbering scheme will be referred to in section III.B.2.

to the S_1 state. Lednev used Monti's potential energy curves to explain his results. Therefore, these transients have been assigned assuming the rotational pathway dominates after S_2 excitation.

Fujino[19] performed time-resolved Raman spectroscopy to show that the S_1 state formed after S_2 excitation had a similar NN stretching frequency as that of the S_0 state. This indicates the NN double bond remains intact after the excitation and therefore provides evidence for the inversion mechanism in the S_1 state. In later work, Fujino[20] presented results from a time-resolved fluorescence experiment that denied the existence of a rotational pathway that starts from the S_2 state, in contrast with Monti's work. They showed that isomerization always occurs in the S_1 state regardless of excitation wavelength. To explain the differing quantum yields, he proposed an additional relaxation channel must be opened upon S_2 excitation that produces mostly trans isomers.

Much theoretical work has been done to investigate the photochemistry of azobenzene. Cattaneo and Persico[21] performed CASSCF and CIPSI calculations to generate potential energy curves of the ground and excited states. Ishikawa et al.[22] obtained three-dimensional potential energy surfaces of the S_0, S_1, S_2, and S_3 state using CASSCF and MRCISD. Quennville[23] used CASSCF to generate potential energy curves for the lowest five electronic states. Tiago et al.[24] performed two-dimensional surface scans for S_0, S_1, and S_2 using TDDFT. Ciminelli et al.[25] used a combination of Tully's surface hopping approach with a direct semiempirical calculation to study the dynamics in the excited states. Cembran et al.[26] calculated the lowest singlet and triplet excited-state PES along the torsion pathway using CASPT2. Gagliardi et al.[27] also focused on the torsion pathway but used MS-CASPT2 and TDDFT. Diau[28] used CASSCF to look at the inversion, rotation, and concerted-inversion pathways on the S_1 surface.

The most recent theoretical conclusions agree that the $n \rightarrow \pi^*$ state has a slight inversion barrier and a nearly barrierless rotation pathway.[21,22,24,25,28,30] Several researchers have found an S_1-S_0 conical intersection along the rotation pathway with an CNNC dihedral angle of $\sim 90.0°$.[22−26,28] It is generally agreed that when excited to the S_1 state, relaxation to the S_0 state occurs through the conical intersection along the midpoint of the rotation pathway.[22,26,28] Recent experimental work has shown support for this mechanism.[29] The comprehensive studies of Fujino and Tahara[19] showed that isomerization does not occur directly on the S_2 state, but that it relaxes to a lower lying excited state, where it then isomerizes. Some calculations point to an S_2-S_1 conical intersection near the *trans*-azobenzene Franck−Condon region which leads to a direct S_2 to S_1 relaxation.[23,25]

Many models have been unable to explain the difference in quantum yield that is seen upon excitation to the S_2 state. Diau proposed a new isomerization pathway that is open after S_2 excitation.[28] This channel produces more trans isomers than cis thereby lowering the trans to cis quantum yield. This mechanism is explored in our studies.

In addition to investigating the preferred isomerization mechanism, we also look at how substituting the phenyl rings of azobenzenes affects the isomerization process. To study these effects, we examined the pathways by generating potential energy surfaces of the ground and excited states of azobenzene [Azo] and four of its derivatives, 4,4′-diaminoazobenzene [Azon], 4,4′-nitro-aminoazobenzene [$AzoNO_2NH_2$], N-[4-(4-(Acetylamino)phenylazo)phenyl]-acetamide [Azonco], and 4,4′-dinitroazobenzene [$AzoNO_2NO_2$] (Figure 2). The azobenzenes will be referred to by the name in brackets throughout the remainder of the paper.

Absorption spectroscopy by Blevins and Blanchard on the Azo, Azon, and Azonco systems suggests that the ground-state isomerization barrier is reduced when electron-donating substituents are placed on the benzene rings.[30] Our results, however, indicate that electron-donating groups, like NH_2 and $HNCOCH_3$, increase the ground-state inversion barrier while electron withdrawing groups, like NO_2, decrease it. Lack of solvent effects in our calculations may be the reason for these discrepancies as will be discussed further in this paper.

II. Computational Details

A. Ground-State Calculations. All calculations were performed using Gaussian 03.[31] All ground-state geometries were computed using ab initio density-functional theory with the B3LYP[32] functional and the 6-31G* basis set[33] as this method was previously found to accurately reproduce experimental

TABLE 1: Optimized Geometries of cis and trans Isomers of Azobenzene

	angles/deg			distances/Å		energy[a]
	∠CNNC	∠NNCC	∠NNC	d_{NN}	d_{CN}	kcal mol^{-1}
trans	180.0	0.0	114.8	1.261	1.419	0.0
trans X-ray[b]	180.0	0.0	114.1	1.247	1.428	
trans ED[c]	180.0	30.0	114.5	1.268	1.427	
cis	9.8	50.3	124.1	1.250	1.436	15.2
cis X-ray[d]	0.0	53.3	121.9	1.253	1.449	

[a] Energies are relative to the trans isomer. [b] Reference 36. [c] Reference 35. [d] Reference 37.

results.[34] To investigate the rotation and inversion pathways, the potential energy surface was generated by scanning the NNC angle (angle φ in Figure 1, angle 7−8−9 in Figure 2) from 80.0° to 180.0° and the CNNC dihedral angle (dihedral angle ϕ in Figure 1, angle 4−7−8−9 in Figure 2) from −40.0° to 220.0° at a 10.0° interval. For each calculation, the NNC angle and the CNNC dihedral angle were fixed at the appropriate values while the rest of the degrees of freedom were optimized. The remaining points in the potential energy surface were found through symmetry. The potential energy surface for the concerted inversion pathway was generated in the same manner with the exception that the NNC and CNN angles were scanned synchronously. Two potential energy surfaces were built for the 4,4′-nitro-aminoazobenzene because of its asymmetrically substituted benzene rings. Azo(NO_2)NH_2 refers to the surface with NO_2 on the same side as the NNC angle being inverted (9−8−7 in Figure 2) while AzoNO_2(NH_2) represents the surface with NH_2 on the same side as the inverted NNC angle (4−7−8 in Figure 2). Charges were calculated using the CHelpG method to extract the electron donating or withdrawing nature of each substituent.

B. Excited-State Calculations. Time dependent density-functional theory (TDDFT) with the B3LYP functional and the 6-31G* basis set were used for the excited-state calculations as they were found to give reliable results[3]. The excited-state potential energy surfaces were generated by calculating single point vertical excitation energies for each of the points in the ground-state potential energy surfaces. All calculations were performed using Gaussian 03.[31]

III. Results and Discussion

A. Unsubstituted Azobenzene. *A.1. Optimized Ground-State Geometry.* The optimized geometries of *cis*- and *trans*-azobenzene were found, and the results are shown in Table 1. The trans isomer is about 15.2 kcal mol^{-1} or 0.66 eV lower in energy than the cis isomer. This is just slightly higher than the experimental value of 0.6 eV[1]. Different experimental methods suggest different structures for the trans isomer. Electron diffraction[35] results indicate the phenyl rings of the trans isomer are 30° out of plane, whereas the X-ray[36] data show a planar structure. Our results agree with the X-ray data as well as with the results of several theoretical calculations.[21,22,26,38] The structure of the cis isomer is less controversial. Our DFT results are very similar to both X-ray data[37] and other theoretical predictions.[21,22,24,26,34,38]

A.2. Electronic Excitation Energies. For the singlet vertical excitations of the trans isomer of azobenzene, the first transition, n → π*, is symmetry forbidden and therefore has a very weak oscillator strength, while the second transition, $\pi \rightarrow \pi$*, is much more intense. The excitation energies for these transitions are shown in Table 2. The assignment of symmetry is done by visual inspection. Evaluation of our molecular orbitals (Figure 3) reveals that the first transition originates from the lone pair on the central nitrogens and is of 88% n → π* character as calculated from the CI coefficients. The second transition is 78% $\pi \rightarrow \pi$* character and is delocalized throughout the entire molecule. It has been suggested that the second excited-state relaxes to the first via a conical intersection above the ground-state trans minimum.

TABLE 2: Vertical Excitation Energies (eV) of trans and cis Azobenzene

		TDDFT[a]	exptl[b]	CASSCF[c]	CIPSI[d]
trans	S_1	2.55 (0.0)	2.79	2.85	2.81
	S_2	3.77 (0.77)	3.95	7.62	4.55
cis	S_1	2.57 (0.04)	2.82	3.65	2.94
	S_2	4.12 (0.07)	4.77	8.62	4.82

[a] Intensity is in parentheses. [b] Reference 3. [c] Reference 22. [d] Reference 21.

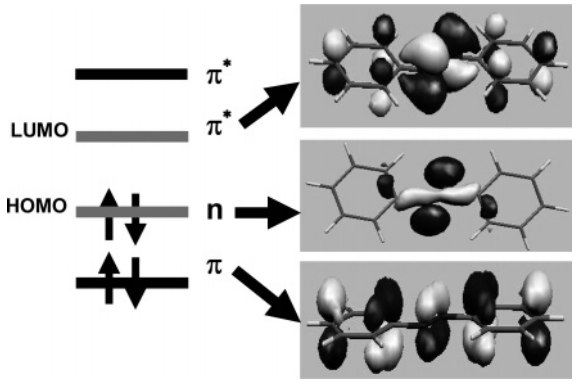

Figure 3. Molecular orbitals of Azo involved in the $S_1 \leftarrow S_0$ and $S_2 \leftarrow S_0$ transitions. This figure also represents the molecular orbitals of Azon and Azonco as they are very similar to those of Azo.

The TDDFT calculated energy for the $S_1 \leftarrow S_0$ transition of *trans*-azobenzene, 2.55 eV, is fairly close to that of the known experimental value, 2.79 eV[3]. Although CASSCF[22] and configuration interaction by perturbative iterative selection (CIPSI)[21] calculations have given values that agree slightly better with experiment for this transition, 2.85 and 2.81 eV, respectively, the $S_2 \leftarrow S_0$ transition is much better described by TDDFT with an energy of 3.77 eV compared to an experimental value of 3.95 eV. CASSCF predicts an energy of 7.62 eV and the CIPSI energy is 4.55 eV. TDDFT consistently predicts slightly lower energies than the experimental values, while the CASSCF values are generally much higher. These values are summarized in Table 2.

The $S_1 \leftarrow S_0$ transition occurs at about the same energy for both trans and cis. Unlike the trans excitations, however, the $S_1 \leftarrow S_0$ transition from the cis isomer shows slight intensity because of the loss of symmetry making the transition allowed. The $S_2 \leftarrow S_0$ transition from the cis isomer is much less intense and slightly higher in energy than that of the trans isomer.

A.3. Potential Energy Surfaces. A.3.a. Ground State. A ground state three-dimensional potential energy surface and a contour map were calculated for azobenzene (Figure 4). The surface is very symmetric with two cis and two trans minima. Cis to trans barrier heights were determined from these plots by finding the energy of the highest point on the potential energy surface along the pathway and subtracting from it the energy of the cis minimum. Proper identification of these points as true transition states was done, checking for the existence of only one imaginary frequency in normal modes analysis. The peak along the inversion pathway (angle reaction coordinate) was taken to be at an angle of 180.0° and a dihedral angle of 180.0° and is

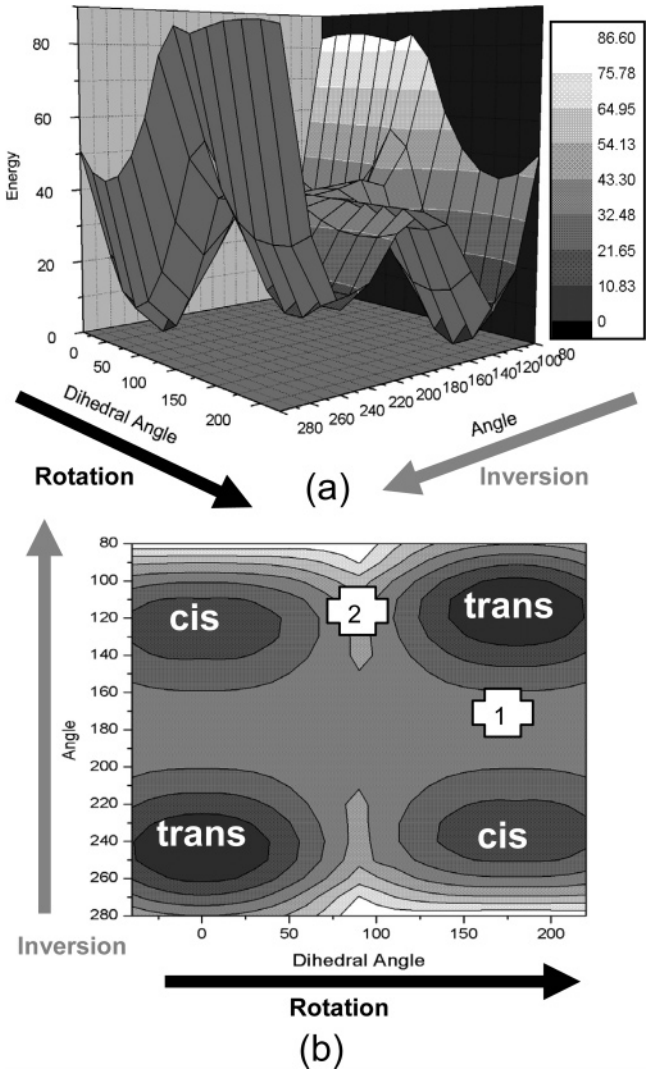

Figure 4. (a) Potential energy surface and (b) contour map of the ground state of Azo. Angles are in degrees and energy is in kcal mol^{-1}, relative to the energy of the ground-state trans isomer. In panel b, point 1 marks the position of the inversion transition state while point 2 indicates the position of the rotation transition state. The cis and trans minima are also labeled.

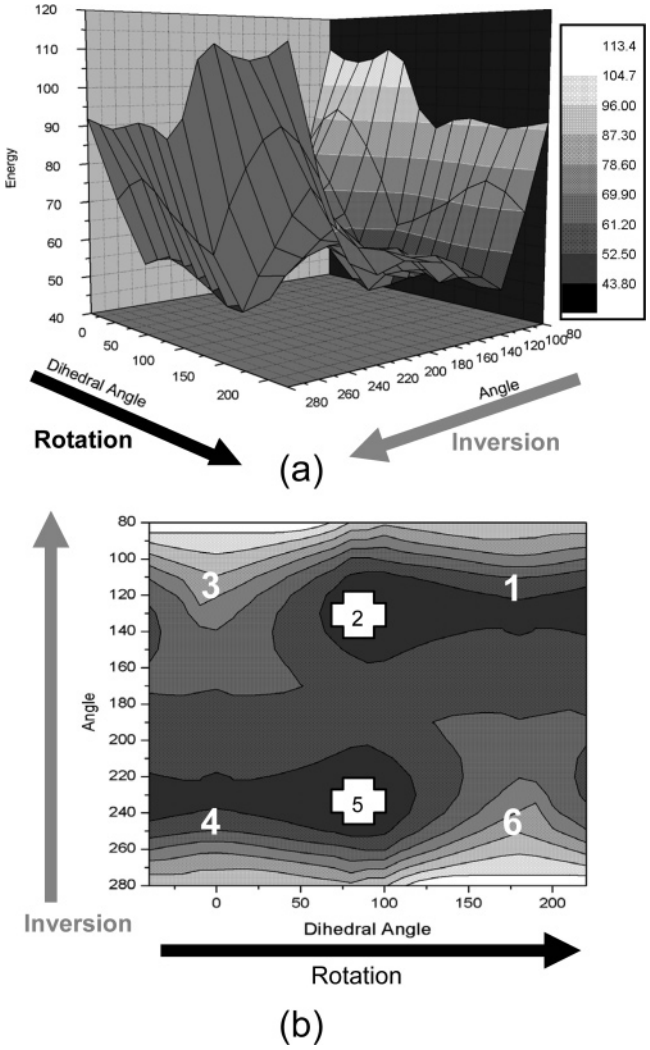

Figure 5. (a) Potential energy surface and (b) contour map of the first excited state of Azo. Points 1 and 4 represent where the molecule is on the S_1 surface after excitation from the ground-state trans minima, whereas excitation from the ground-state cis minima will place in the molecule at points 3 and 6. Points 2 and 5 represent the S_1 minima as well as mark the location of the S_1/S_0 conical intersection. Angles are in degrees and energy is in kcal mol^{-1}, relative to the energy of the ground-state trans isomer.

represented in Figure 4b by point 1. The peak of the rotational pathway (dihedral angle reaction coordinate) was taken to be at a dihedral angle of 90.0° while the angle was the same as that of the trans minimum, 110.0°. In the rotation pathway, the peak was a saddle point and is labeled point 2 in Figure 4b.

Azobenzene is known to undergo a thermal cis to trans isomerization in the ground state so only the cis barriers will be discussed. The barrier along the inversion pathway, 24.9 kcal mol^{-1}, was lower than that of the rotation pathway, 36.2 kcal mol^{-1}, indicating that in the ground state, the inversion mechanism is favored. This is in agreement with previous reports.[15,21,30,39] A cis to trans barrier height for azobenzene was measured experimentally[30] to be 25.8 kcal mol^{-1}, in good agreement with our results.

We can explain the difference in energy barriers between mechanisms by looking at how the NN distance changes along each pathway. Along the inversion pathway, the NN distance decreases (increases in bond order) from the trans isomer to the transition state (point 1 in Figure 4b) and then increases in length (decreases in bond order) as it approaches the cis isomer. The inversion transition state shows the strongest NN bond along the pathway. The opposite trend is seen along the rotation pathway. The NN distance increases from the trans isomer to the rotation transition state (point 2 in Figure 4b) and then decreases in length as it approaches the cis isomer. The NN distance found in the rotation transition state is approximately that of a single bond. There is a high energy cost involved in a decrease of the NN bond order in the rotation pathway which is seen as an increase in the energy barrier.

A.3.b. Excited State 1 (n $\rightarrow \pi^*$). Potential energy surfaces and contour maps were calculated for the first two excited states (Figure 5). Our surfaces are similar to those of previous calculations.[22,24] Vertical excitations from the trans minima reach the points labeled 1 and 4 while excitations from the cis minima arrive at the points labeled 3 and 6. Points 2 and 5 depict the placement of the S_1 minima.

A.3.b.1. Rotation Pathway. There is essentially no energy barrier along the rotation pathway of the first excited state as has also been reported in previous calculations.[21,22,24,25,28,30] The potential energy surface along this pathway has only a shallow slope above the area corresponding to the trans minimum (from points 1 to 2 and 4 to 5 in Figure 5b), 0.21 kcal (mol·degree)$^{-1}$, and a very steep slope on the cis side (from points 3 to 2 and

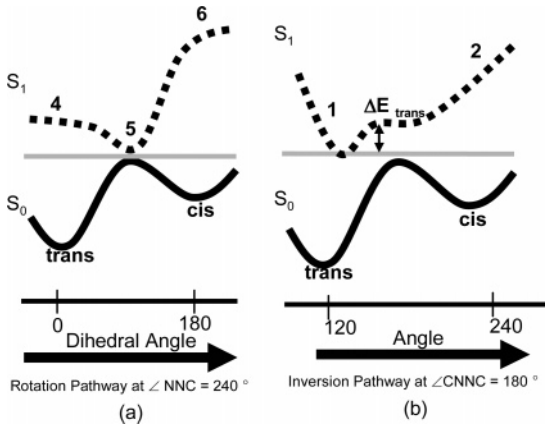

Figure 6. Schematic representation of (a) the rotation pathway and (b) the inversion pathway in the first excited state. The curves in panel a are along the angle of 240°, while those in panel b are along the dihedral of 180°. The labeled points are the same as those in Figure 5b. The arrow in b depicts the inversion barrier in the S_1 state.

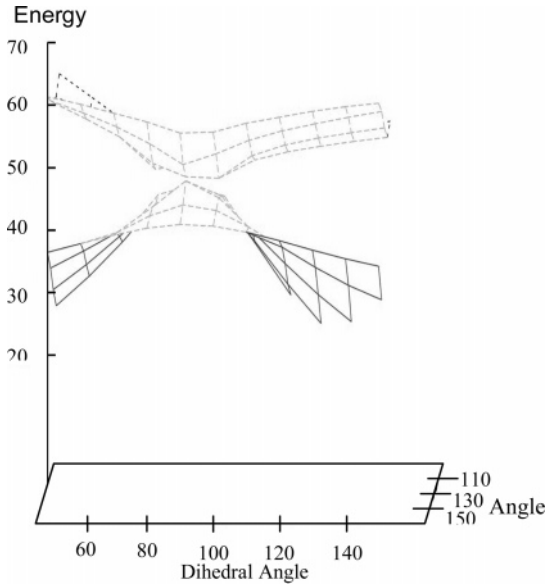

Figure 7. Conical intersection of S_0 and S_1 states of Azo. Angles are in degrees and energy is in kcal mol^{-1}.

6 to 5 in Figure 5b), 0.33 kcal (mol·degree)$^{-1}$. These slopes are also shown schematically in Figure 6. The figures suggest that when excited from the cis conformation there is a much faster relaxation to the excited state minimum than if excited from the trans conformation. This phenomenon has been shown experimentally by femtosecond transient absorption measurements.[40]

A conical intersection was found between the ground and first excited states. It can be seen when the minimum of the excited state is very close in energy to the maximum barrier height along the rotation pathway in the ground state as can be seen in Figure 7. We have located our conical intersection at an NNC angle of 140.0 and a CNNC dihedral angle of 90.0 (point 5 in Figures 5b and 6a). The location of this conical intersection is in agreement with several other groups.[22−26,28] The splitting between the surfaces is estimated to be 0.65 kcal mol^{-1}.

Stilbene, which can only isomerize via the rotation mechanism, has been found to have an S_1-S_0 conical intersection along the midpoint of the rotation pathway and is also known to have an isomerization yield of 0.5. It is interesting to find that azobenzene has a conical intersection near the same location yet shows a very different quantum yield. This can be explained by looking at the difference in slope on the S_1 surface on either side of the conical intersection in azobenzene. As mentioned previously, the S_1 slope above the cis minimum (point 6 in Figure 6) is greater than the corresponding slope on the trans side (point 4 in Figure 6). The crossing probability close to the conical intersection can be related to the nonadiabatic coupling between S_0 and S_1[41] written as

$$d_{S_1-S_0} = \langle \varphi_{S_0} | \nabla \varphi_{S_1} \rangle$$

A larger slope corresponds to a larger change in wave function (right side of formula). There is a greater probability, therefore, of jumping from S_1 to S_0 when starting from the cis side rather than the trans side resulting in more trans isomers in the S_0 state, since the transition carries the momentum from the excited state. In other words, while oscillating on the S_1 surface near the conical intersection, more relaxation occurs when the wave packet moves from point 6 to point 5 than from point 4 to point 5, depositing more population on the trans side than on the cis side of the ground-state surface, hence producing a quantum yield lower than 0.5. The slopes (cis and trans sides) on the S_1 surface of stilbene are essentially equal giving rise to more similar S_0 and S_1 wave functions than those of azobenzene. The probability of jumping from S_1 to S_0 is equal when coming from either side of the conical intersection in the case of stilbene. This results in the experimentally seen quantum yield of 0.5.

A.3.b.2. Inversion Pathway**.** There is a slight trans → cis energy barrier along the inversion pathway as can be seen in Figure 6. The S_1 trans → cis energy barrier is 9.6 kcal mol^{-1}. There is no conical intersection between the ground and first excited state along this pathway making the inversion mechanism highly improbable. This is in agreement with previous calculations.[23,28]

Our results indicate that the isomerization can easily occur through an excitation to the first excited state, relaxation to the excited-state minimum along the rotation pathway, followed by descent to either the cis or trans conformation via the conical intersection, providing for the known cis yield (0.20−0.36) after excitation to the first excited state.

A.3.c. Excited State 2 ($\pi \rightarrow \pi^*$). The potential energy surfaces of the second excited state are shown in Figure 8. As in the ground-state surface, cis and trans minima appear on the surface of the S_2 state along the inversion and rotation pathways. The cis minima are extremely shallow. The trans → cis energy barriers were computed in the same manner as the ground-state cis → trans barriers. The inversion barrier was found to be 30.1 kcal mol^{-1}, while that of the rotation pathway was 29.6 kcal mol^{-1}. Because of these substantial energy barriers, it is unlikely that isomerization occurs on the S_2 surface. Rapid relaxation from the S_2 state to the S_1 state is energetically more favorable. This is in agreement with Kasha's rule.[42] We examined energy gaps between the two states along the inversion, rotation, and concerted inversion pathways in order to investigate this process.

A.3.c.1. Rotation Pathway. The possibility of a conical intersection between the S_2 and S_1 states along the rotation pathway with an angle of 117° and a dihedral angle of 180° has been previously suggested.[23] For Azo, the states differ by 23.48 kcal mol^{-1} at the trans minimum as can be seen in Figure 9a. We do not find a conical intersection between S_1 and S_2 along the rotation pathway and can therefore rule out this pathway as an isomerization mechanism.

A.3.c.2. Inversion Pathway. A conical intersection between the S_2 and S_1 states has been previously located near the ground-state trans minima.[25] While we do not find a curve crossing in

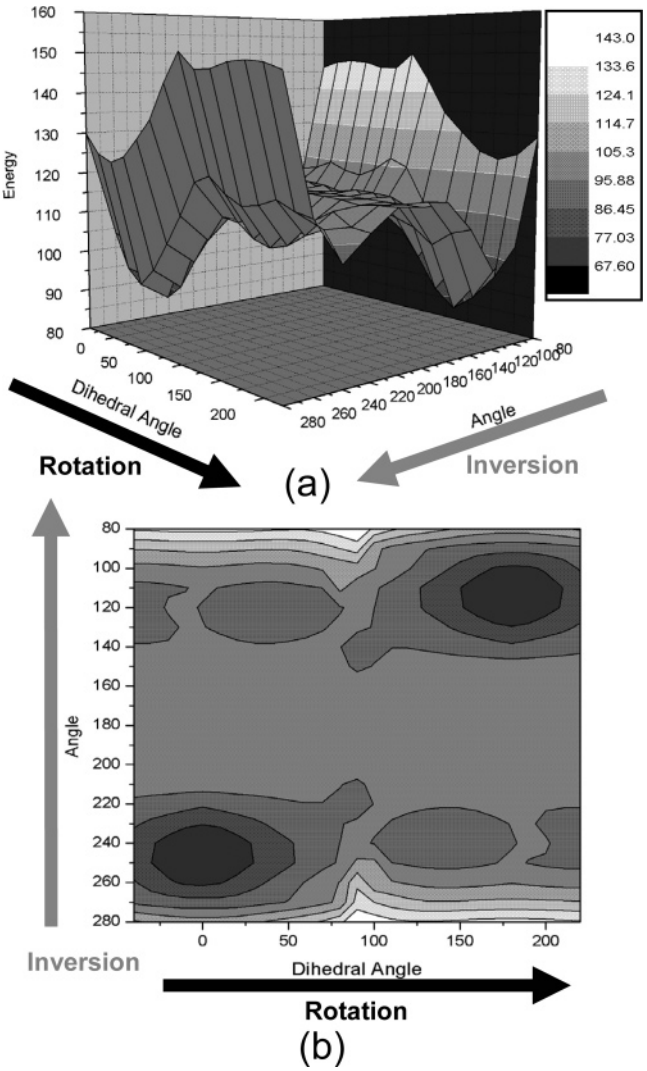

Figure 8. (a) Potential energy surface and (b) contour map of the second excited state of Azo. Angles are in degrees and energy is in kcal mol^{-1}, relative to the energy of the trans isomer.

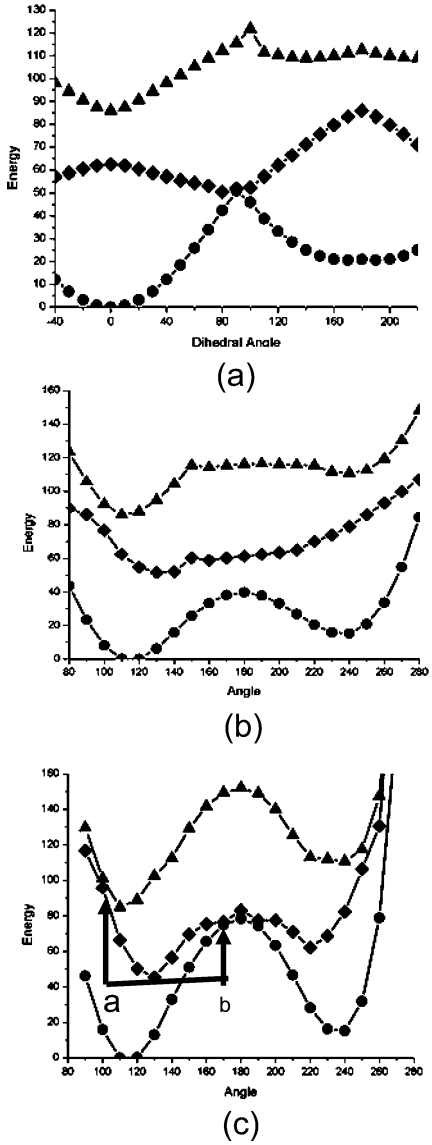

Figure 9. (a) Rotation pathway along the angle of the ground-state minimum of Azo, ∠NNC = 110°; (b) inversion and (c) concerted-inversion pathways of Azo along ∠CNNC = 180.0 °: S_0 in closed circles, S_1 in diamonds, S_2 in triangles. Angles are in degrees and energy is in kcal mol^{-1}. In panel c, arrow a represents the available energy, whereas arrow b represents the energy barrier.

this exact area, we do see the energy difference between the S_1 and S_2 states become smaller along the inversion pathway as can been seen in Figure 9b. This point is a few degrees away from the S_2 minima. At a CNNC dihedral angle of 180.0° and an NNC angle of 100.0°, the energy gap between the S_1 and S_2 surfaces appears to be the smallest, 15.70 kcal mol^{-1}. This energy gap may be small enough to allow for rapid relaxation to the first excited state. This explains why experimentalists see two transients, a shorter one corresponding to the S_2 state before it relaxes to a longer lived species corresponding to the S_1 state[16−18].

A.3.c.3. Concerted Inversion Pathway. The above mechanism does not explain the difference in quantum yield that is seen upon excitation at different wavelengths for unsubstituted azobenzene. To explain this process, we invoke Diau's[28] proposal of an additional isomerization channel (concerted-inversion) that is opened by exciting to the S_2 state. The concert-inversion pathway involves a synchronous inversion of the NNC and CNN angles. In our calculations, the CNNC dihedral angle is fixed at 180.0°. The concerted inversion pathway is plotted in Figure 9c.

As in the inversion pathway, the S_1 and S_2 surfaces are close in energy at an NNC angle of 100.0°. This energy gap is significantly smaller than that of the rotation or inversion pathway, 5.17 kcal mol^{-1}. It seems likely that rapid relaxation from the S_2 to S_1 state can occur because of this small energy gap which will again give rise to two transients as seen experimentally. A potential problem of the concerted-inversion mechanism is the existence of an energy barrier on the S_1 surface. The energy barrier (labeled b in Figure 9c) is measured by subtracting the energy of the S_1 minimum from the S_1 energy at the S_1-S_0 conical intersection, 31.21 kcal mol^{-1}. The available energy is calculated by subtracting the S_1 minimum energy from the S_1 energy at the S_2-S_1 conical intersection (labeled a in Figure 9c), 50.43 kcal mol^{-1}. There is enough energy available to overcome the energy barrier so the channel is open.

A.4. Summary of Azo. Excitation to the S_1 state leads to isomerization via the rotation mechanism. Our conclusion is based on the finding of a conical intersection between the S_1 and S_0 states near the midpoint of this pathway (NNC = 110, CNNC = 90.0). The rotation pathway has also been found to be without a significant barrier, unlike the inversion pathway.

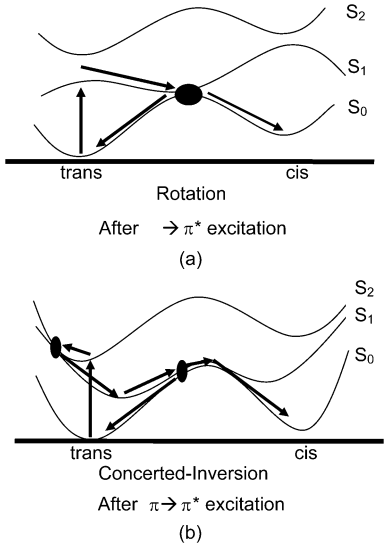

Figure 10. Scheme of the trans → cis isomerization process after (a) n → π^* excitation and (b) $\pi \rightarrow \pi^*$ excitation. The ovals indicate locations of curve crossings.

Excitation to the S_2 state results in rapid relaxation to the S_1 surface via the conical intersection found at NNC = 100 and CNNC = 180 along the concerted inversion pathway. The energy gap between these surfaces is significantly smaller than those seen in other pathways. Once on the concerted-inversion S_1 surface there is an energy barrier of approximately 31.2 kcal mol^{-1}. Only when excitation to the S_2 state occurs is there enough energy to overcome this barrier. The conical intersection between the S_1 and S_0 states is located at NNC = 170 and CNNC = 180. More trans isomers would be produced because the crossing of these states is on the trans side of the potential energy curve. This is in agreement with the experimental observation of differing quantum yields upon excitations at different wavelengths. The concerted-inversion pathway has a nearly planar transition state in which the NN double bond stays intact. This explains Fujino's observation that the S_1 state formed after S_2 excitation had a similar NN stretching frequency as that of the S_0 state.[19] It should also be noted that because the S_2 state relaxes to the S_1 state at a geometry similar to that of both the electronic ground state as well as the direct S_1 excited state in the Franck−Condon region, the spectra of both S_1 states should be quite similar as seen in Fujino's work.[43] A schematic diagram of these mechanisms is shown in Figure 10.

TABLE 3: Optimized Geometries of cis and trans Isomers of Azobenzenes

	structure	angles/deg ∠CNNC	∠NNCC	∠NNC	distances/Å R_{NN}	R_{NC}	energy[a] kcal mol^{-1}
trans	Azo	180.0	0.0	114.8	1.261	1.419	0
	Azon	180.0	0.1	115.0	1.267	1.409	0
	Azonco	180.0	0.0	114.9	1.265	1.411	0
	$Azo(NO_2)NH_2$	179.9	0.2	114.1	1.267	1.415	0
	$AzoNO_2(NH_2)$	179.9	0.0	115.6	1.267	1.399	0
	$AzoNO_2NO_2$	179.9	0.2	114.6	1.260	1.427	0
cis	Azo	9.8	50.3	124.1	1.250	1.436	15.2
	Azon	11.8	44.1	124.6	1.256	1.430	16.8
	Azonco	11.1	46.0	124.5	1.253	1.431	16.1
	$Azo(NO_2)NH_2$	11.5	60.4	125.5	1.254	1.423	15.6
	$AzoNO_2(NH_2)$	11.5	30.4	125.0	1.254	1.419	15.6
	$AzoNO_2NO_2$	10.2	52.2	124.0	1.247	1.432	14.8

[a] Energies are relative to their respective trans minima.

B. Substituted Azobenzenes. *B.1. Optimized Ground-State Geometry.* The optimized geometries of the cis and trans isomers of the azobenzenes were found using the same technique as for the unsubstituted azobenzene. Important bond distances, angles, and dihedrals are summarized in Table 3. The values listed for

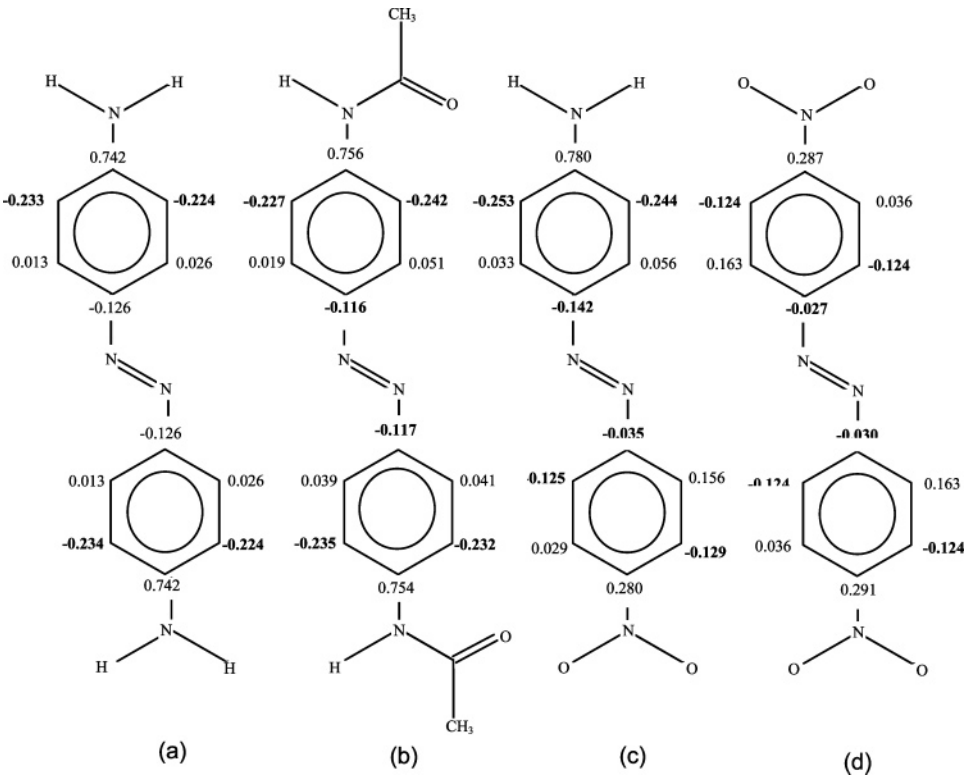

Figure 11. Comparison of charge differences in trans isomers (a) Azon, (b) Azonco, (c) $AzoNO_2NH_2$, (d) $AzoNO_2NO_2$. Charge differences were calculated by subtracting the charge on the unsubstituted azobenzene from that of the substituted azobenzene. A negative charge difference (highlighted in bold) indicates that the position has been activated.

TABLE 4: Vertical Excitation Energies in eV of *trans*- and *cis*-Azobenzenes

		$S_1 \leftarrow S_0$ ($n \rightarrow \pi^*$)			$S_2 \leftarrow S_0$ ($\pi \rightarrow \pi^*$)			$S_2 \leftarrow S_0 - S_1 \leftarrow S_0$
structure		energy	intens	% $n \rightarrow \pi^*$[a]	energy	intens	% $\pi \rightarrow \pi^*$[a]	energy difference
trans	Azo	2.55	0.0	88	3.77 (3.96[b])	0.77	79	1.22
	Azon	2.71	0.0	89	3.26 (3.15[b])	1.03	78	0.55
	Azonco	2.59	0.0	88	3.25 (3.41[b])	1.29	80	0.66
	$AzoNO_2NH_2$	2.44	0.0	85	2.99	0.86	80	0.55
	$AzoNO_2NO_2$	2.31	0.0	86	3.48	1.07	80	1.17
cis	Azo	2.57	0.04	78	4.12	0.07	87	1.55
	Azon	2.46	0.09	71	3.70	0.22	77	1.24
	Azonco	2.46	0.10	74	3.72	0.29	73	1.26
	$AzoNO_2NH_2$	2.46	0.11	60	3.17	0.09	40	0.71
	$AzoNO_2NO_2$	2.44	0.07	75	3.62	0.03	81	1.18

[a] The % $n \rightarrow \pi^*$ and % $\pi \rightarrow \pi^*$ values are calculated from the CI coefficients. [b] Reference 30, experimental value.

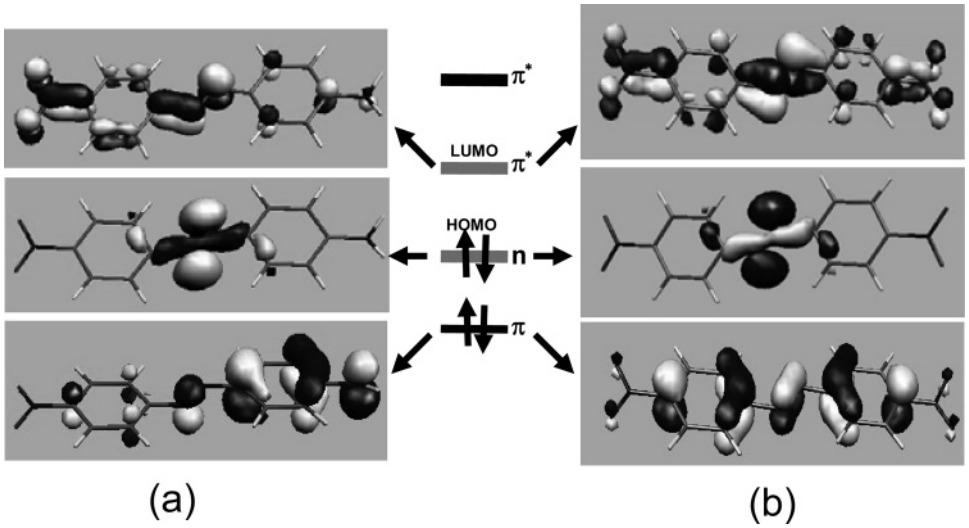

Figure 12. (a) Molecular orbitals of $AzoNO_2NH_2$ involved in the $S_1 \leftarrow S_0$ and $S_2 \leftarrow S_0$ transitions. (b) Molecular orbitals of $AzoNO_2NO_2$ involved in the $S_1 \leftarrow S_0$ and $S_2 \leftarrow S_0$ transitions.

$Azo(NO_2)NH_2$ are those of the NO_2 substituted ring, while the values for NH_2 substituted ring are represented by $AzoNO_2(NH_2)$.

B.1.a. NN Distance. For each azobenzene studied, the NN bond is shorter for the cis isomer than the trans isomer. The NN distances were quite similar between the azobenzenes ranging from 1.260 to 1.267 Å for the trans isomer and 1.247 to 1.256 Å for the cis isomer. $AzoNO_2NO_2$ has the shortest NN distance for both conformations followed by Azo. The substituents appear to contribute only slightly to the NN bond as evidenced by the very small increase in bond length upon substitution of the rings with electron donating groups and a small decrease in length when substituted with electron withdrawing groups.

B.1.b. NNC Angle, CNNC Dihedral Angle, and NNCC Dihedral Angle. Like the NN distances, the NNC angles are very similar. For the trans conformation, the angles range from 114.1° to 115.6°, while the range for the cis isomer was from 124.0° to 125.5°. The CNNC dihedral angles of the trans isomers are all about the same, 180.0° while the NNCC dihedral angles were about 0.0°. The CNNC dihedral angle for the cis isomers is slightly larger in substituted azobenzenes ranging from 9.8° for Azo to 11.8° for Azon. The NNCC dihedral angle was smallest for $AzoNO_2(NH_2)$ and largest for $Azo(NO_2)NH_2$.

B.1.c. Relative Energy Differences. The difference between the cis and trans ground-state energies was calculated and found to be very similar ranging from 14.8 kcal mol^{-1} for $AzoNO_2NO_2$ to 16.8 kcal mol^{-1} for Azon. Electron donating substituents appeared to increase the relative energy difference while electron withdrawing groups lowered the energy difference. The push−pull system showed a slight increase in relative energy difference when compared to Azo.

B.2. Comparison of Charges. We define electron donating groups as those that activate the ortho and para positions while electron withdrawing groups are those that activate the meta positions. Activation is determined by change in charges relative to the unsubstituted azobenzene. Blevins and Blanchard[30] suggested the CH_3CONH groups of Azonco would act as electron withdrawing substituents. Using the charges from electrostatic potentials (CHELPG) method to calculate charges, however, we found that Azonco demonstrates electron donating behavior similar to that of Azon. The charge differences were calculated by subtracting the charge on the unsubstituted azobenzene from that of the substituted azobenzene. As can be seen in Figure 11, the carbons that are ortho to the substituent, C2, C6, C11, and C13, (refer to numbering scheme in Figure 2) have similar charge differences with an average of −0.226 for Azon and −0.234 for Azonco. The para carbons, C4 and C9, are only slightly activated with average charge differences of −0.126 for Azon and −0.117 for Azonco. The activation of the ortho carbons is enhanced by the electron withdrawing effect of the azo group. The azo group activates the positions meta to itself, which are the same as those ortho to the substituent. In effect, the azo group will act synergistically with the electron donating substituents.

Interesting behavior results when an electron donating substituent, NH_2, is placed on one benzene ring para to the azo group and an electron withdrawing group, NO_2, is placed in

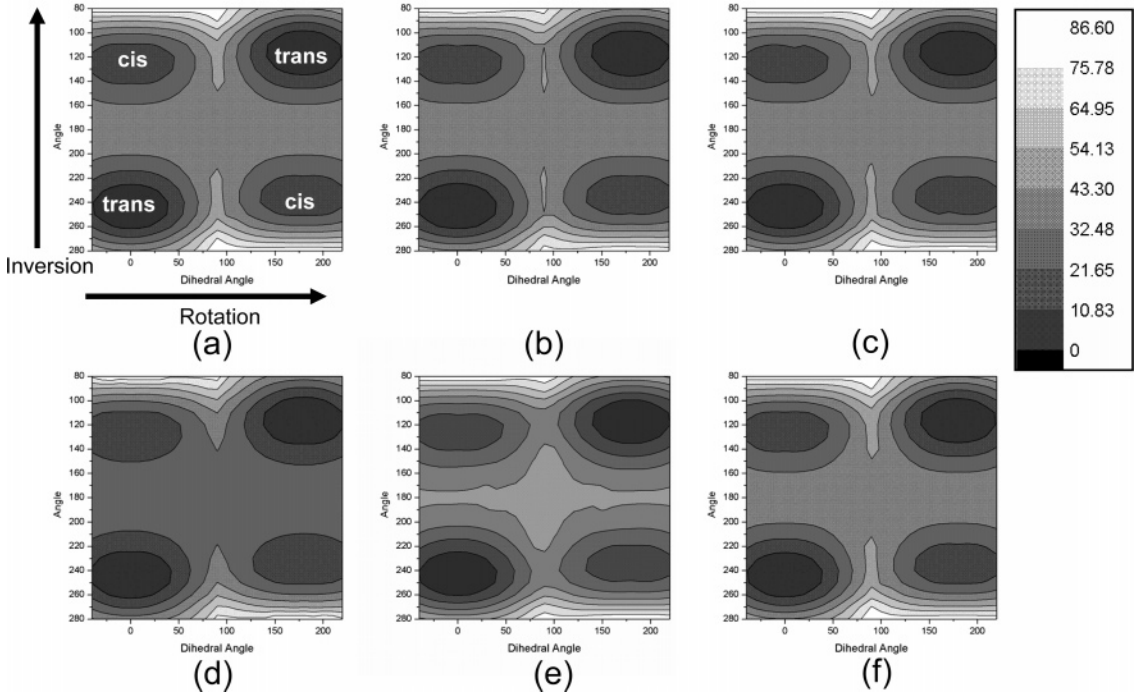

Figure 13. Contour maps of the ground state of (a) Azo, (b) Azon, (c) Azonco, (d) Azo(NO_2)NH_2, (e)AzoNO_2(NH_2), and (f) AzoNO_2NO_2. Angles are in degrees, energy is in kcal mol^{-1}.

TABLE 5: The cis → trans Energy Barriers Calculated along the Inversion (inv) and Rotation (rot) Pathways[a]

	Azo		Azon		Azonco		Azo(NO_2)NH_2		AzoNO_2(NH_2)		AzoNO_2NO_2	
	inv	rot	inv	rot	inv	rot	inv	rot	inv	rot	inv	rot
∠NNC	180	110	180	120	180	110	180	110	180	120	180	120
∠CNNC	180	90	180	90	180	90	180	90	180	90	180	90
$\Delta E^{\ddagger}_{cis}$	24.9	36.2	26.8	30.5	25.5	34.2	17.2	31.6	28.5	20.8	20.8	29.2
$\Delta\Delta E^{\ddagger b}$	11.3		3.7		8.7		3.6				8.4	

[a]Angles are in degrees. [b] $\Delta\Delta E^{\ddagger}$ is the energy difference in kcal mol^{-1} between the rotation and inversion isomerization barriers.

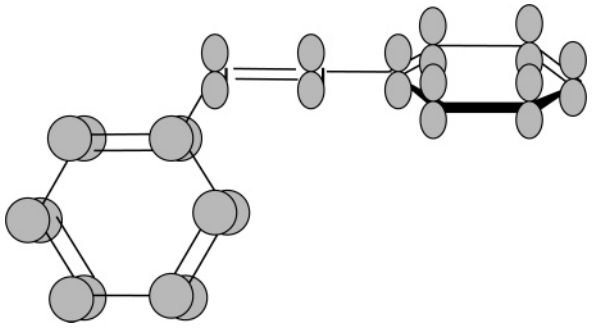

Figure 14. Schematic diagram of the molecular orbitals of the inversion transition state.

the para position of the other benzene ring. This creates a push−pull system as in AzoNO_2NH_2. As seen in Azon, the NH_2 group activates the positions ortho to itself, C2 and C6, which are the same as those positions meta to the azo group as depicted in Figure 3. When an electron withdrawing group like NO_2 is placed on the ring para to the azo group, there is a mixing of charges. Both groups try to activate the positions that are meta with respect to themselves. This will obviously result in a conflict because the meta positions of the azo group are ortho to the NO_2 group. What we see is a difference in charge of −0.125 at C14, which is meta to the NO_2 group, and −0.129 at C11, which is meta to the azo group. Therefore C11 and C14 are the activated carbons in AzoNO_2NH_2. AzoNO_2NO_2 also shows a mixing of charges. Similar results are seen in AzoNO_2-NO_2; C3, C6, C11, and C14 are activated.

TABLE 6: Dipole Moments (in Debye) of the Inversion Transition State (TS) and cis Isomer

	dipole moment cis	dipole moment inversion TS
Azo	3.22	3.22
Azon	2.61	4.44
Azonco	5.35	7.39
Azo(NO_2)NH_2	7.53	13.37
AzoNO_2(NH_2)	7.53	8.79
AzoNO_2NO_2	3.66	5.89

It can now be stated with confidence that Azonco and Azon have electron donating groups, AzoNO_2NO_2 had electron withdrawing groups and Azo(NO_2)NH_2 is a push−pull system with both an electron donating and an electron withdrawing group.

B.3. Electronic Excitation Energies. The singlet vertical excitations of the trans isomers of the substituted azobenzenes are very similar to unsubstituted azobenzene. The first transition, n → π^*, is symmetry forbidden and therefore has a very weak oscillator strength, while the second transition, $\pi \rightarrow \pi^*$, shows some intensity. Visual inspection is used to assign symmetry.

The excitation energies for the $S_0 \leftarrow S_1$ transition for all the azobenzenes were similar, as shown in Table 4. The molecular orbitals (Figures 3 and 12) show again that the first transition originates from the lone pair on the central nitrogens. Figure 3 can be used to represent the molecular orbitals for Azo, Azon, and Azonco. The excitation was of nearly pure n → π^* character for all but AzoNO_2NH_2 and AzoNO_2NO_2. These systems show some additional charge transfer to their NO_2 substituents.

The second transition, $\pi \rightarrow \pi^*$, is delocalized throughout the entire molecule for all but the push−pull system. $AzoNO_2NH_2$ shows an excitation primarily from the π orbitals of the benzene ring with the NH_2 substituent as well as from the π orbitals of the central nitrogens. As in the $n \rightarrow \pi^*$ transition, $AzoNO_2NH_2$ and $AzoNO_2NO_2$ both show a charge transfer to the NO_2 substituents. The molecular orbitals involved in the second transition are pictured in Figures 3 and 12.

$AzoNO_2NH_2$ exhibits an intense trans excitation with the smallest energy, 2.99 eV, while the $\pi \rightarrow \pi^*$ excitations of Azonco and Azon are particularly close in energy, 3.25 and 3.26 eV, respectively. $AzoNO_2NO_2$ has an excitation of 3.48 eV. The $S_2 \leftarrow S_0$ transition of Azo is highest in energy, 3.77 eV, and the least intense of all the azobenzenes. It appears that adding both electron donating and electron withdrawing substituents to Azo decreases the excitation energy and increases the intensity of the $S_2 \leftarrow S_0$ transition.

We have found again that the first and second excited states at the optimized ground-state trans geometry are very close in energy. Azo shows the largest energy gap, 1.22 eV, followed by $AzoNO_2NO_2$, 1.17 eV, and Azonco, 0.66 eV. Azon and $AzoNO_2NH_2$ have very similar energy gaps, 0.550 and 0.546 eV, respectively. The energy differences between the first two excited states are summarized in Table 4.

The energy of the steady-state absorption spectroscopy maximum of Azo was 3.96 eV,[30] slightly higher than the TDDFT maximum of 3.77 eV. Azon showed an experimental excitation of 3.15 eV, while the calculated energy was 3.26 eV. Azonco showed an excitation of 3.41 eV, slightly higher than the calculated energy of 3.25 eV. Both experimental and theoretical results show Azo to have the highest energy transition. TDDFT predicts the excitation energies of Azon and Azonco to be about the same, while experiment shows these energies to differ by 0.26 eV.

It is also interesting to compare differences between the cis and trans excitations. Unlike the trans excitations, the $S_1 \leftarrow S_0$ transition from the cis isomer shows slight intensity. For Azo and $AzoNO_2NH_2$, the $S_1 \leftarrow S_0$ transition occurs at about the same energy for both trans and cis. Azon and Azonco have trans $S_1 \leftarrow S_0$ excitations slightly higher in energy than cis excitations, while $AzoNO_2NO_2$ shows a higher energy cis excitation.

The $S_2 \leftarrow S_0$ transition from the cis isomer is much less intense and slightly higher in energy than that of the trans isomer. There is a greater difference between the cis and trans $S_2 \leftarrow S_0$ transitions than the $S_1 \leftarrow S_0$ transitions. The greatest difference is seen in Azonco with almost 0.5 eV separating the cis and trans excitations.

B.4. Potential Energy Surface. B.4.a. Ground State. Ground-state three-dimensional potential energy surfaces and contour maps were calculated for each azobenzene (Figure 13). As mentioned previously, for the push-pull system, $Azo(NO_2)NH_2$ represents the surface with NO_2 on the same side as the NNC angle being inverted while $AzoNO_2(NH_2)$ represents the surface with NH_2 on the same side as the inverted NNC angle. As can be seen in these figures, the ground-state surfaces of the azobenzenes are very similar. Cis to trans barrier heights were determined as described in section III.A.3.a. The energy barriers can be found in Table 5. For the push-pull system, the barriers for both $Azo(NO_2)NH_2$ and $AzoNO_2(NH_2)$ were considered together.

In all five systems, the barrier along the inversion pathway was lower than that of the rotation pathway, indicating that in the ground state, the inversion mechanism is still favored. The unsubstituted azobenzene, Azo, was found to have an inversion barrier of 24.9 kcal mol^{-1}. $Azo(NO_2)NH_2$ and $AzoNO_2NO_2$ have barriers lower than Azo, 17.2 kcal mol^{-1} and 20.8 kcal mol^{-1}, respectively. In both of these systems, the inversion angle is adjacent to a phenyl ring with an electron withdrawing substituent. Azonco, Azon, and $AzoNO_2(NH_2)$ each have an electron donating substituent on the phenyl ring adjacent to the inversion angle and showed higher barriers than Azo at 25.5 kcal mol^{-1}, 26.8 kcal mol^{-1}, and 28.5 kcal mol^{-1}, respectively. It is clear from our results that substituting the benzene ring attached to the angle being inverted with an electron donating group raises the inversion barrier height compared to the unsubstituted azobenzene. Substituting the same ring with an electron withdrawing group lowers the barrier height. These observations can be explained upon examination of the molecular orbitals of the inversion transition state (Figure 14).

Each of the azobenzenes has an inversion transition state with an angle of 180° and a dihedral angle of 180°. Because of the electron donating substituents on Azon and Azonco, there is more electron density on the phenyl rings than is seen on Azo. There is therefore greater steric hindrance between the lone pairs on the central nitrogens and p orbitals of the phenyl ring adjacent to the 180° NNC angle. The steric effects cause the inversion transition state of Azon and Azonco to be higher in energy than that of Azo. $AzoNO_2NO_2$, on the other hand, has electron withdrawing substituents which accept electron density from the π orbitals of the phenyl rings. $AzoNO_2NO_2$ is slightly stabilized by the ability of the less filled π orbitals of the phenyl ring adjacent to the 180° NNC angle to accept electron density from the lone pair orbitals of the central nitrogens. The lower barrier height of $AzoNO_2NO_2$ compared to Azo is due to this stabilization.

For the push−pull system, the smallest barrier appears along the inversion pathway of $Azo(NO_2)NH_2$. This suggests that the preferred mechanism of isomerization in the ground state of the push−pull system is the inversion of the NNC angle that is on the same side as the NO_2 substituent. This is in agreement with the results of Kikuchi's[44] studies of a similar push−pull system, 4-(dimethylamino)-4′-nitroazobenzene. This system has the lowest inversion energy barrier of all the azobenzenes studied. The transition state is stabilized by the vacant orbitals of the nitro substituted phenyl rings accepting electron density from the lone pairs on the central nitrogens. The lone pairs are parallel to the vacant π orbitals on this phenyl ring. The lone pairs are also perpendicular to the occupied orbitals of the amine substituted phenyl ring which has a stabilizing effect as it minimizes the electron−electron repulsion. The combination of these effects results in the $Azo(NO_2)NH_2$ having the lowest inversion energy barrier.

Blevins and Blanchard looked at the ground state cis → trans back-conversion for Azo, Azon, and Azonco using theory and experiment. They calculated barrier heights from their experimentally measured isomerization recovery time constants. The experiments did not indicate which pathway the barriers referred to, so we will compare them to both the inversion and rotation cis to trans barriers. A barrier height of 21.2 kcal mol^{-1} was measured for Azon, 23.7 kcal mol^{-1} for Azonco, and 25.8 kcal mol^{-1} for Azo. The experimental data indicate that adding electron donating substituents decreases the energy barrier which conflicts with our results. This may be due to the lack of consideration of solvent effects in our calculations. The dipole moment of the cis isomer and the transition state will be stabilized by the polar solvent. The dipole moments were calculated and can be found in Table 6. For Azo, the cis isomer and the inversion transition state have approximately the same

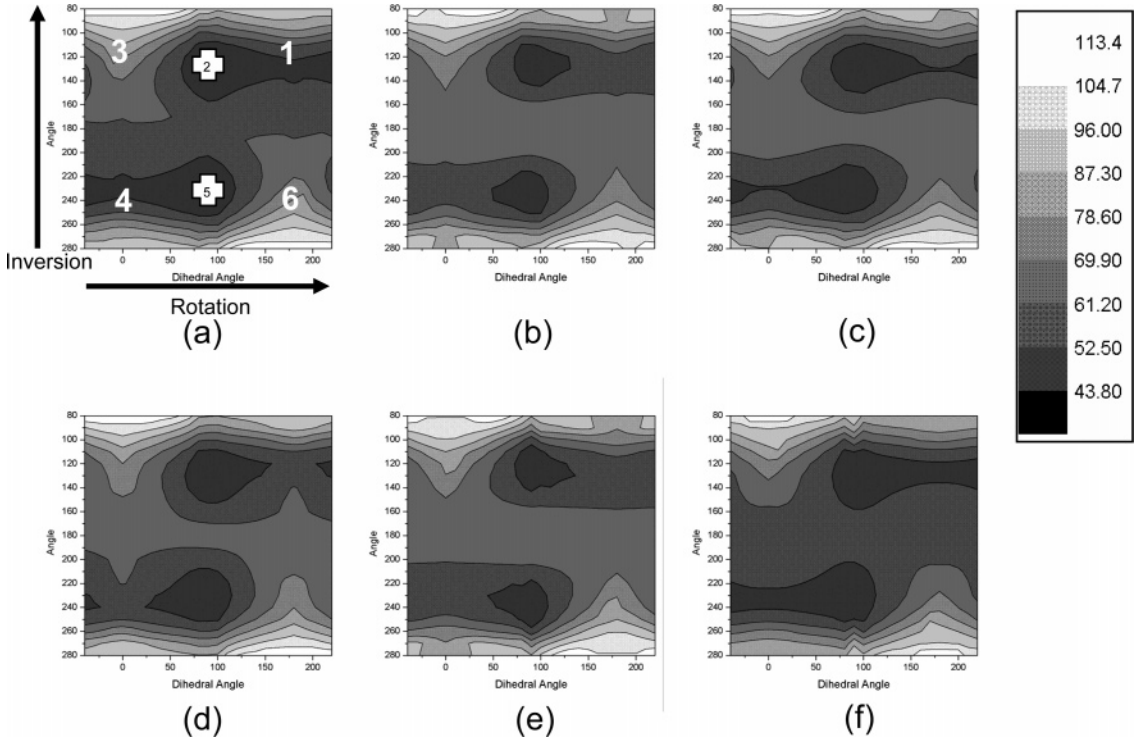

Figure 15. Contour maps of the first excited state of (a) Azo, (b) Azon, (c) Azonco, (d) $Azo(NO_2)NH_2$, (e) $AzoNO_2(NH_2)$, (f) $AzoNO_2(NO_2)$. Angles are in degrees, energy is in kcal mol^{-1}.

TABLE 7: NN Distances (Å) of the Transition States along the Rotation and Inversion Pathways

	inversion	rotation
Azo	1.226	1.303
Azon	1.241	1.308
Azonco	1.233	1.322
$Azo(NO_2)NH_2$	1.228	1.335
$AzoNO_2(NH_2)$	1.248	1.290
$AzoNO_2NO_2$	1.222	1.297

TABLE 8: Rotational Energy Barriers in the First Excited State[a]

	trans barrier	cis barrier
Azo	18.5 (0.206)	29.8 (0.331)
Azon	11.6 (0.129)	28.6 (0.318)
Azonco	19.2 (0.213)	29.2 (0.324)
$Azo(NO_2)NH_2$	17.5 (0.194)	31.1 (0.346)
$AzoNO_2(NH_2)$	13.9 (0.154)	32.0 (0.356)
$AzoNO_2NO_2$	11.5 (0.128)	27.3 (0.303)

[a] This barrier is measured as the difference in energy between the excited-state minimum and the excited state point corresponding to the ground-state trans and cis minima. Energies are in kcal mol^{-1}; the slope, in parentheses, is in units of kcal mol^{-1} $degree^{-1}$.

TABLE 9: The Placement and Energy of the First Excited State Minimum Involved in the Conical Intersection

	angles/deg		energy[a]
	∠NNC	∠CNNC	kcal mol^{-1}
Azo	140	90	46.0
Azon	130	90	47.0
Azonco	130	100	43.9
$Azo(NO_2)NH_2$	140	90	42.4
$AzoNO_2(NH_2)$	120	90	38.9
$AzoNO_2NO_2$	150	90	45.4

[a] Energies are relative to their respective trans ground-state minimum.

TABLE 10: The trans → cis Inversion Energy Barriers in the First Excited State[a]

	ΔE_{trans}
Azo	9.6
Azon	11.1
Azonco	1.3
$Azo(NO_2)NH_2$	2.3
$AzoNO_2(NH_2)$	11.5
$AzoNO_2NO_2$	10.4

[a] These barriers were found by subtracting the energy of the excited state point above the ground-state trans minimum from the energy of the excited state at an angle of 180.0° and a dihedral of 180.0°. Energies are in kcal mol^{-1}.

dipole moment indicating they will be equally stabilized by a polar solvent. This may explain why our calculated barrier height is closest to the experimental value for Azo. The inversion transition states of Azon and Azonco are more stabilized by a polar solvent than their corresponding cis isomers because of their greater dipole moment. Stabilization of the transition state will lower the energy barrier as is seen when comparing our calculated results with experiment. Polar solvents will have the greatest effect on the push−pull system owing to the large dipole moments that can be found in both the transition state as well as the cis isomer.

The NN distance changes along each pathway in the substituted azobenzenes follow the same trend seen for unsubstituted azobenzene (see section III.A.3). Along the inversion pathway, the NN distance is smallest at the transition state. The values of the NN distances in the transition states can be found in Table 7. The inversion transition state of $AzoNO_2NO_2$ has the shortest NN distance, 1.222 Å, followed by Azo, 1.226 Å, and $Azo(NO_2)NH_2$, 1.228 Å. The inversion transition state of Azonco was found to have an NN distance of 1.233 Å while that of Azon was found to be 1.241 Å. $AzoNO_2(NH_2)$ had the longest NN distance, 1.248 Å. The electron donating groups can contribute electron density to the π^* orbitals thereby decreasing the bond order and increasing the length of the NN

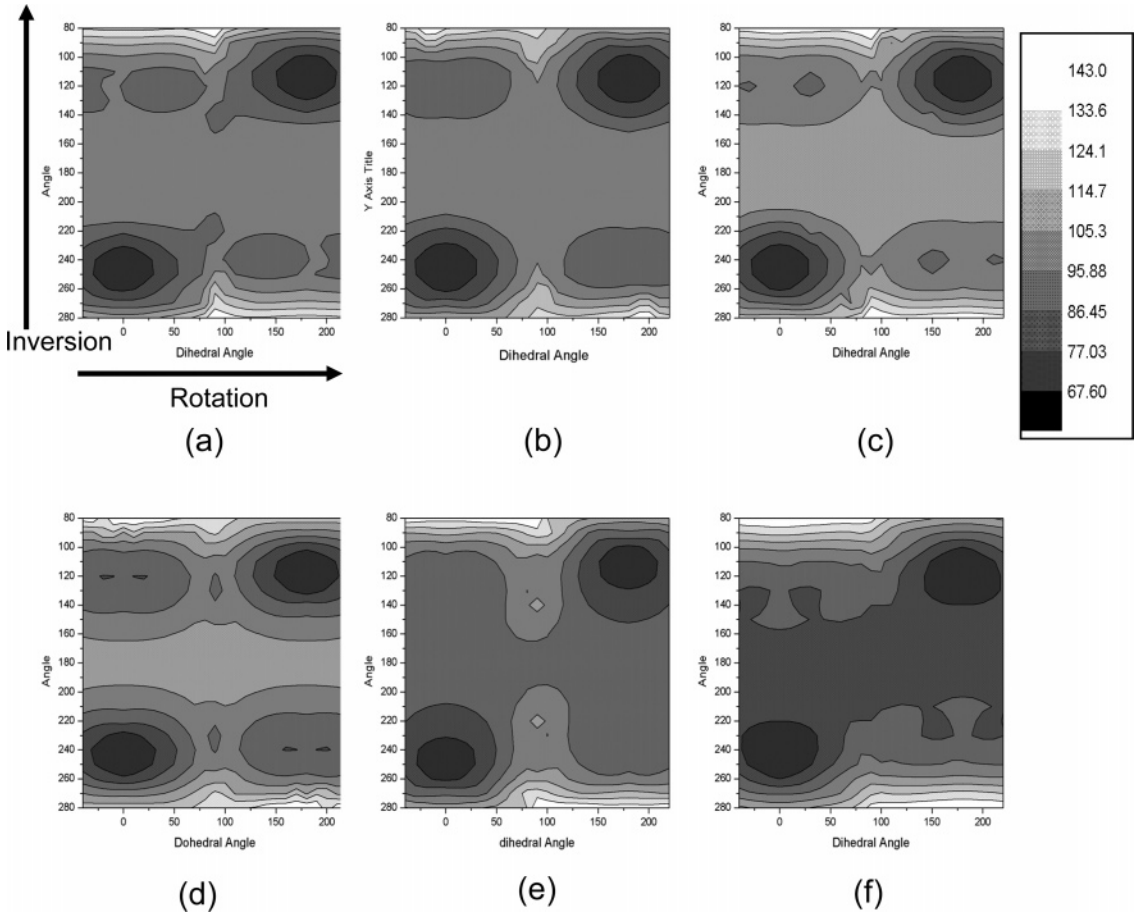

Figure 16. Contour maps of the second excited state of (a) Azo, (b) Azon, (c) Azonco, (d) Azo(NO_2)NH_2, (e) AzoNO_2(NH_2), (f) AzoNO_2NO_2. Angles are in degrees, energy is in kcal mol^{-1}.

TABLE 11: The trans → cis Energy Barriers Calculated along the Inversion (inv) and Rotation (rot) Pathways on the Second Excited State Surface[a]

	Azo		Azon		Azonco		Azo(NO_2)NH_2		AzoNO_2(NH_2)		AzoNO_2NO_2	
	inv	rot	inv	rot	inv	rot	inv	rot	inv	rot	inv	rot
∠NNC	180	110	180	110	180	120	180	120	180	110	180	110
∠CNNC	180	90	180	90	180	90	180	90	180	90	180	90
$\Delta E^{\ddagger}_{trans}$	30.1	29.6	40.5	46.2	40.2	34.9	43.1	28.4	27.1	31.1	14.5	27.7
$\Delta\Delta E^{\ddagger}$[b]	0.5		5.7		5.3		1.3				13.2	

[a] Angles are in degrees. Energies are in kcal mol^{-1}. [b] $\Delta\Delta E^{\ddagger}$ is the energy difference between the rotation and inversion isomerization barriers.

bond compared to that of the unsubstituted azobenzene. These distances indicate that the central nitrogens of the inversion transition state have a double bond between them.

The opposite trend is seen along the rotation pathway, the NN distance is greatest at the transition state and is approximately that of a single bond. These distances can also be found in Table 7. Azo(NO_2)NH_2 has the longest NN bond distance, 1.335 Å, while AzoNO_2(NH_2) has the shortest NN distance, 1.290 Å.

B.4.b. Excited State 1. Potential energy surfaces and contour maps were calculated for the first two excited states. Figure 15 shows these calculations for the first excited state of all the azobenzenes. The surface graphs of all substituted azobenzenes appear to be similar to Azo (Figure 5) and are therefore not shown. Slight differences are more visible in the contour plots.

B.4.b.1. Rotation Pathway. As seen in unsubstituted azobenzene, there is essentially no energy barrier along the rotation pathway of the first excited state. There is a shallow slope above the area corresponding to the trans minimum and a very steep slope on the cis side. We can compare the excited-state cis and trans energy barriers and slopes (Table 8) to approximate relative relaxation times. A steeper slope indicates a quicker relaxation time. We can conclude from this analysis that the lifetime of the first excited-state cis isomer is shorter than that of the trans for each of the azobenzenes studied here. Azonco appears to have the steepest trans slope and we predict it will exhibit the

TABLE 12: Energy Differences between S_1 and S_2 for the Rotation, Inversion, and Concerted-Inversion Pathways[a]

	energy gap at $A = 110°$ $D = 180°$ (rotation)	energy gap at $D = 180°$ $A = 100°$ (inversion)	energy gap at $D = 180°$ $A = 100°$ (concerted-inversion)[b]
Azo	26.43	15.70	5.17
Azon	22.06	0.69	2.79
Azonco	17.12	3.56	6.24
Azo(NO_2)NH_2	8.89	4.67	3.49
AzoNO_2(NH_2)	17.30	2.30	3.49
AzoNO_2NO_2	22.83	16.01	6.36

[a] Energies are in kcal mol^{-1}. [b] For the concerted-inversion pathway, Azo(NO_2)NH_2 and AzoNO_2(NH_2) are the same.

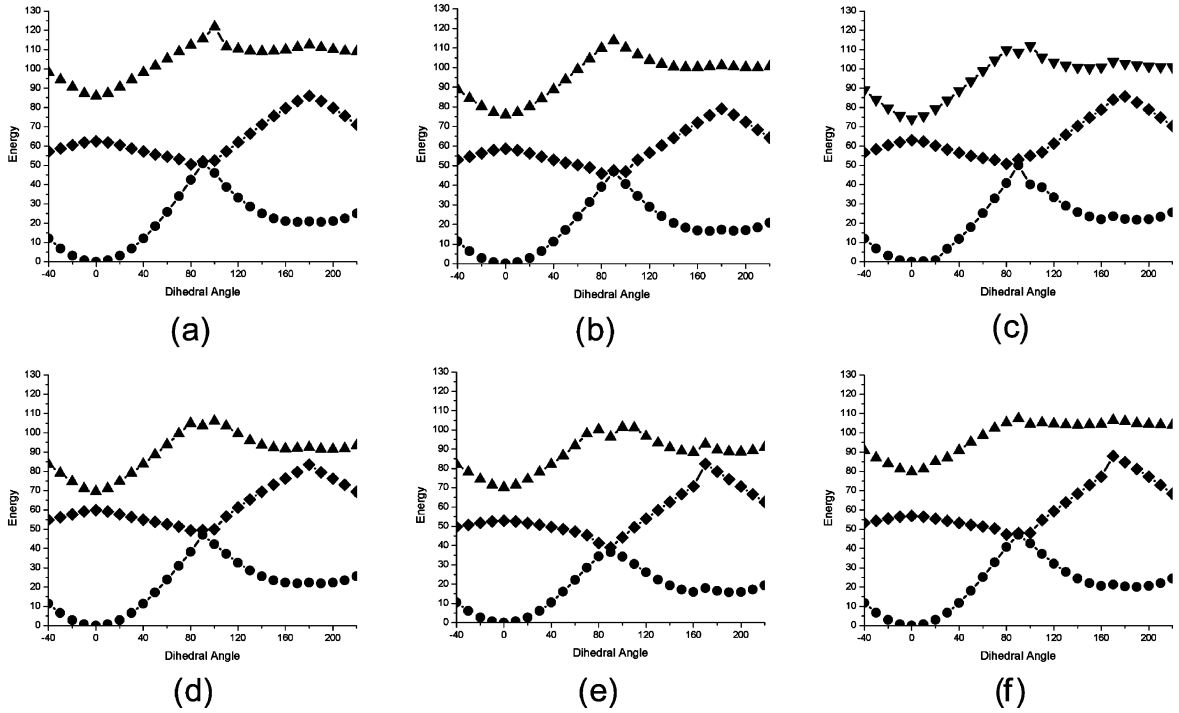

Figure 17. Rotation pathway along the angle of the ground-state minimum of (a) Azo, (b) Azon, (c) Azonco, (d) $Azo(NO_2)NH_2$, (e) $AzoNO_2(NH_2)$, (f) $AzoNO_2NO_2$. Angles are in degrees, energy is in kcal mol^{-1}.

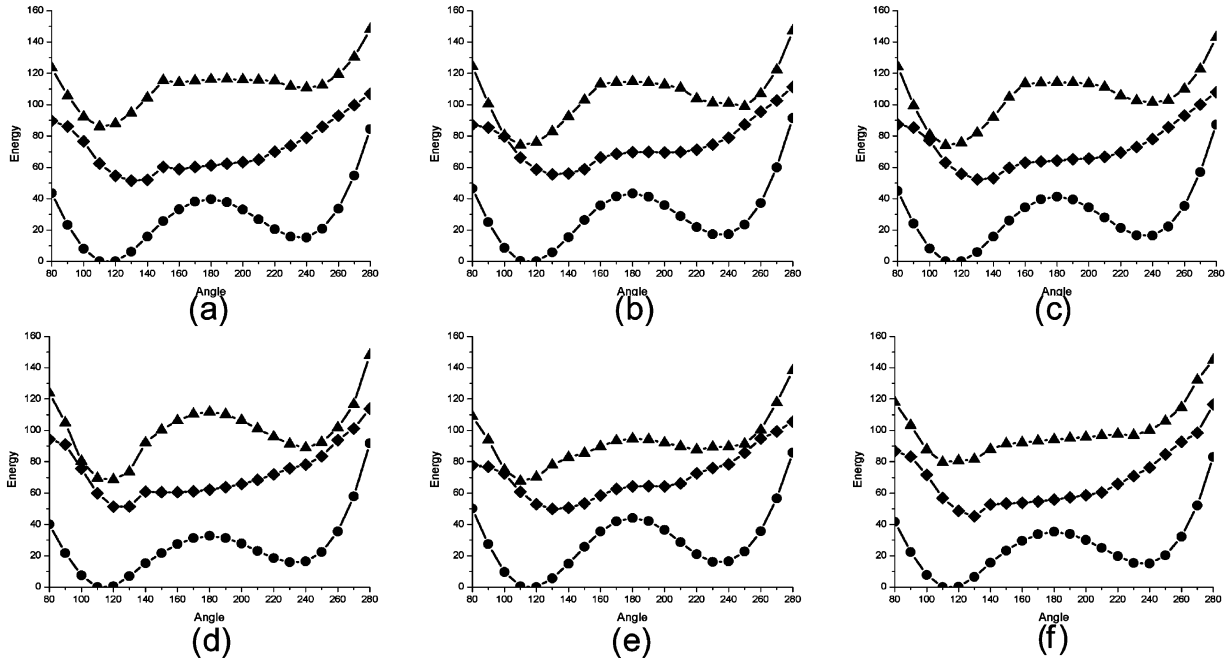

Figure 18. Inversion pathway along the dihedral of the ground-state minimum of (a) Azo, (b) Azon, (c) Azonco, (d) $Azo(NO_2)NH_2$, (e) $AzoNO_2(NH_2)$, (f) $AzoNO_2NO_2$. Angles are in degrees, energy is in kcal mol^{-1}.

shortest S_1 lifetime, while $AzoNO_2NO_2$ has the least steep slope and is expected to have the longest S_1 lifetime.

A conical intersection was discovered in each azobenzene between the ground and first excited states. The location of the conical intersection is only slightly different between the azobenzenes. The location as well as the relative energy can be found in Table 9. Azonco's conical intersection is located on the trans side of the barrier. This may indicate that Azonco will have a lower cis → trans quantum yield.

B.4.b.2. Inversion Pathway. We again see a trans → cis energy barrier along the inversion pathway (Table 10). $AzoNO_2(NH_2)$, Azon, $AzoNO_2NO_2$, and Azo have higher barrier heights, 11.5 kcal mol^{-1}, 11.1 kcal mol^{-1}, 10.4 kcal mol^{-1}, and 9.6 kcal mol^{-1}, respectively. $Azo(NO_2)NH_2$ and Azonco show very small inversion barriers, 1.3 kcal mol^{-1} and 2.3 kcal mol^{-1}, making it difficult to rule out this pathway as a possible isomerization mechanism for these azobenzenes on the basis of barrier height alone. Lack of a conical intersection between the ground and first excited state along this pathway makes the inversion mechanism highly improbable. We can conclude that substituting the phenyl rings of azobenzene does not change the isomerization mechanism after S_1 excitation.

B.4.c. Excited State 2. The potential energy surfaces of the second excited state were also generated and can be found in

TABLE 13: Energies of the S_1 and S_2 Minima, Conical Intersections, Barrier Heights, and Available Energy[a]

	S_2 min	S_2 at S_1-S_2 CI	S_1 min	S_1 at S_0-S_1 CI	S_1 barrier[b]	available energy[c]
Azo	84.95	100.99 (5.17)	45.39	76.60 (1.64)	31.21	50.43
Azon	73.19	73.19 (2.79)	49.68	77.63 (6.78)	27.95	20.72
Azonco	73.27	73.27 (6.24)	46.11	81.58 (4.56)	35.47	20.92
$Azo(NO_2)NH_2$	67.72	67.72 (3.49)	41.79	71.12 (2.57)	29.33	22.44
$AzoNO_2NO_2$	79.28	98.78 (6.35)	38.53	72.23 (7.12)	33.70	53.90

[a] Energies are in kcal mol^{-1} and are relative to their respective trans minimum. The numbers in parentheses refer to the energy gaps between the two states. [b] The S_1 barrier is measured as the difference between the S_1 minimum energy and the S_1 energy at the S_0-S_1 conical intersection. [c] The available energy is the difference between the energy of S_1 at the S_2-S_1 conical intersection and the energy of the S_1 minimum. If the available energy is greater than the S_1 barrier, the concerted-inversion channel can be used.

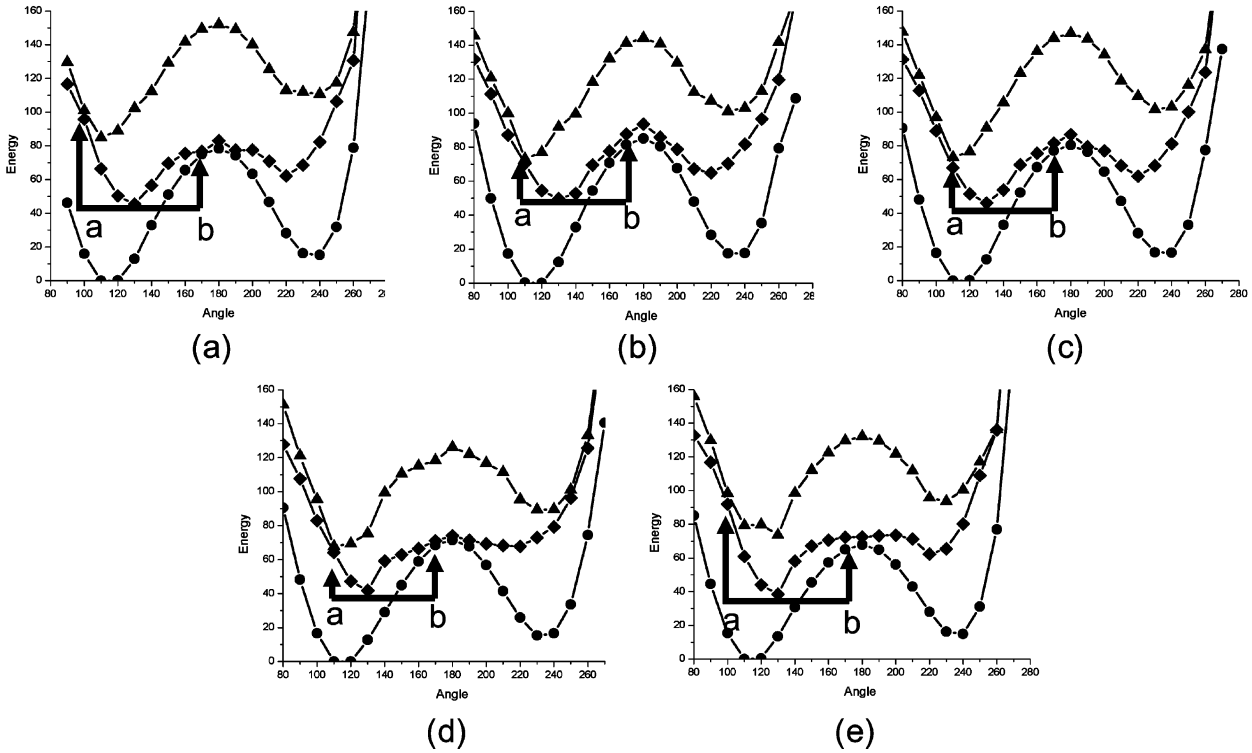

Figure 19. Concerted-inversion pathway along the dihedral of the ground state minimum of (a) Azo, (b) Azon, (c) Azonco, (d) $AzoNO_2NH_2$, (e) $AzoNO_2NO_2$. Angles are in degrees, energy is in kcal mol^{-1}. Only one graph is necessary for $AzoNH_2NO_2$ because the NNC and CNN angles are being scanned synchronously. Arrow a represents the amount of available energy while arrow b represents the energy barrier. The concerted-inversion pathway is only open when the amount of available energy (arrow a) is greater than the energy barrier (arrow b).

Figure 16. Both cis and trans minima appear on this surface along the inversion and rotation pathways of each of the azobenzenes. The trans → cis energy barriers were computed as described previously and can be found in Table 11. These barrier heights are too substantial for isomerization to occur on this surface. Rapid relaxation from the S_2 to the S_1 surface is again expected. We will compare the energy gaps between the first and second excited states along the rotation, inversion, and concerted inversion pathways.

B.4.c.1. Rotation Pathway. As depicted in Figure 17, in general, there is a significant decrease in the energy gap upon substitution of the benzene rings by both electron donating and electron withdrawing groups in agreement with experimental work.[45] These values can be found in Table 12. For Azo, the states differ by 23.48 kcal mol^{-1} above the trans minimum. $Azo(NO_2)NH_2$ shows the smallest energy gap of 8.89 kcal mol^{-1}. These energy gaps are still slightly too high for relaxation to occur along this pathway.

B.4.c.2. Inversion Pathway. The energy difference between the states becomes smaller along the inversion pathway near the trans minima as can been seen in Figure 18 and Table 13. These points are a few degrees away from the minima of the second excited state. In general, at a dihedral angle of 180.0° and angles of 100.0°, the energy gap between the first and second excited-state surfaces appears to be the smallest. Azo and $AzoNO_2NO_2$ have the largest energy gaps, 15.70 kcal mol^{-1} and 16.01 kcal mol^{-1}, respectively. The other azobenzenes show significantly smaller energy gaps, under 4.67 kcal mol^{-1}, making this a very probable pathway.

B.4.c.3. Concerted-Inversion Pathway. This pathway is depicted in Figure 19. Energies of the S_1 and S_2 minima, conical intersections, barrier heights, and available energy can be found in Table 13.

B.4.d. Azon, Azonco, and $AzoNO_2NH_2$. For these three azobenzenes, excitation to the S_2 surface in the franck-condon region results in excitation to the S_2 minimum at NNC = 110.0 and CNNC = 180. This is also the location of the smallest S_2-S_1 energy gap along this pathway, 2.79 kcal mol^{-1} for Azon, 6.24 kcal mol^{-1} for Azonco, and 3.49 kcal mol^{-1} for $AzoNO_2NH_2$. These energy gaps are extremely small and would allow for rapid relaxation from the S_2 surface to the S_1 surface.

As seen in unsubstituted azobenzene, a large energy barrier is seen on the S_1 surface of each of these systems. The energy barriers were measured by subtracting the energy of the S_1

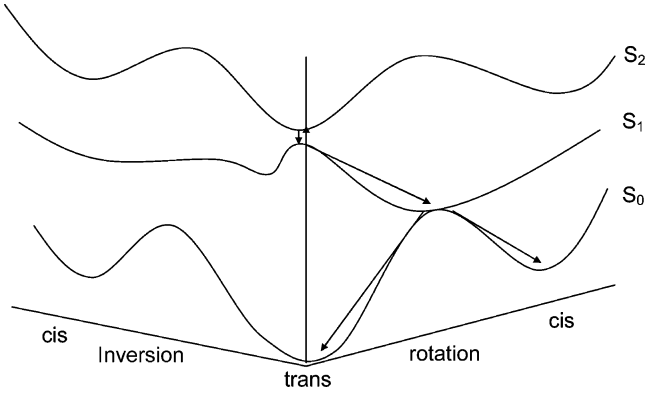

Figure 20. Scheme of the trans → cis isomerization process for Azon, Azonco, and $AzoNO_2NH_2$. After both n → π^* and $\pi \rightarrow \pi^*$ excitation, the rotation pathway dominates the isomerization process.

minimum from the S_1 energy at the S_1-S_0 conical intersection (arrow b in Figure 19). The available energy is calculated by subtracting the S_1 minimum energy from the S_1 energy at the S_2-S_1 conical intersection (arrow a in Figure 19). In each case, the available energy is less than the energy barrier. It is highly improbable that this channel is open for Azon, Azonco, and $AzoNO_2NH_2$. However, highly polar solvents may lower the S_1 energy at the S_1-S_0 conical intersection, which may lower the energy barrier enough to allow for the opening of this channel.

B.4.e. $AzoNO_2NO_2$. $AzoNO_2NO_2$ is quite similar to Azo. The smallest S_1-S_2 energy gap of 6.35 kcal mol^{-1} is found at NNC = 100.0° and CNNC = 180.0°. This energy gap is smaller than that of the rotation and inversion pathways. The available energy was calculated to be 53.90 kcal mol^{-1} while the barrier was found to be 33.70 kcal mol^{-1}. There appears to be sufficient energy to overcome the barrier. More trans isomers would be formed as the S_1-S_0 conical intersection appears at NNC = 170.0° and CNNC = 180.0°.

B.5. Summary of Substituted Azobenzenes. As seen for Azo, the rotation pathway dominates the isomerization process after excitation to the S_1 surface as evidenced by the conical intersection between the S_1 and S_0 states near the midpoint of this pathway (NNC = 110, CNNC = 90.0) and the lack of a significant barrier. Azon, Azonco, and $AzoNH_2NO_2$ use the rotation pathway after excitation to the S_2 state as represented schematically in Figure 20. There is not enough available energy for these azobenzenes to overcome the concerted-inversion barrier. It may be possible for this channel to open in very polar solvents if the transition state is stabilized. The concerted-inversion channel is open for $AzoNO_2NO_2$, after excitation to the S_2 surface.

IV. Conclusions

We have found that adding electron donating substituents to the benzene rings of azobenzene raises the ground-state inversion barrier height, making it harder to isomerize. Electron withdrawing groups were found to lower the same barrier. On the potential energy surface of the first excited state, there exists a slight trans → cis barrier along the inversion pathway, while all other pathways are without barriers. A conical intersection between the S_0 and S_1 states was found for each azobenzene along the rotation pathway making this pathway the most likely method of isomerization. The surface of the S_2 state was shown to be extremely close in energy to the S_1 state at specific points, indicating that excitation to the S_2 state leads to rapid relaxation to the S_1 state. Our results indicate this relaxation occurs using the concerted-inversion pathway for Azo and $AzoNO_2NO_2$. The concerted-inversion energy barriers were too high for the other azobenzenes to overcome. They most likely use the conical intersection found along the rotation pathway as their primary isomerization mechanism, regardless of excitation wavelength.

Acknowledgment. This work was supported in part by DOE Contract DE-F602-02ER45995 and a University of Florida Alumni Fellowship. Computer resources were provided by the Large Allocations Resource Committee through Grant TG-MCA05S010. We also want to thank the anonymous reviewer for insightful comments and pointing out the different quantum yields for azobenzene and stilbene. A.E.R. wishes to thank Sebastian Fernandez-Alberti for very useful discussions on nonadiabatic crossings.

References and Notes

(1) Schulze, F. W.; Petrick, H. J.; Cammenga, H. K.; Klinge, H. *Z. Phys. Chem. Neue Fol.* **1977**, 107.
(2) Talaty, E. R.; Fargo, J. C. *Chem. Commun.* **1967**, *2*, 65.
(3) Rau, H. In *Photochromism: Molecular and Systems*; Durr, H., Bouas-Lauran, H., Eds.; Elsevier: Amsterdam, 1990; p 165.
(4) Liu, Z. F.; Hashimoto, K.; Fujishima, A. *Nature* **1990**, *347*, 658.
(5) Ikeda, T.; Tsutsumi, O. *Science* **1995**, *268*, 1873.
(6) Sekkat, Z.; Dumont, M. *Appl. Phys. B* **1992**, *54*, 486.
(7) Hugel, T.; Holland, N. B.; Cattani, A.; Moroder, L.; Seitz, M.; Gaub, H. E. *Science* **2002**, *296*, 1103.
(8) Muraoka, T; Kinbara, K.; Kobayashi, Y.; Aida, T. *J. Am. Chem. Soc.* **2003**, *125*, 5612.
(9) Zhang, C.; Du, M.-H.; Cheng, H.-P.; Zhang, X.-G.; Roitberg, A. E.; Krause, J. L. *Phys. Rev. Lett.* **2004**, *92*, 1583011.
(10) Bortollus, P.; Monti, S. *J. Phys. Chem.* **1979**, *83*, 648.
(11) Zimmerman, G.; Chow, L.-Y.; Paik, U.-J. *J. Chem. Phys.* **1958**, *80*, 3528.
(12) Rau, H. *J. Photochem.* **1984**, *26*, 221.
(13) Rau, H.; Luddecke, E. *J. Am. Chem. Soc.* **1982**, *104*, 1616.
(14) Bortollus, P.; Monti. S. *J. Phys. Chem.* **1987**, *91*, 5046.
(15) Monti, S.; Orlandi, G.; Palmieri, P. *Chem. Phys.* **1982**, *71*, 87.
(16) Lednev, I. K.; Ye, T.-Q.; Hester, R. E.; Moore, J. N. *J. Phys. Chem.* **1996**, *100*, 13338.
(17) Lednev, I. K.; Ye, T.-Q.; Matousek, P.; Towrie, M.; Foggi, P.; Neuwahl, F. V. R.; Umpathy, S.; Hester, R. E.; Moore, J. N. *Chem. Phys. Lett.* **1998**, *290*, 68.
(18) Lednev, I. K.; Ye, T.-Q.; Abbot, L. C.; Hester, R. E.; Moore, J. N. *J. Phys. Chem. A* **1998**, *102*, 9161.
(19) Fujino, T.; Tahara, T. *J. Phys. Chem. A* **2000**, *104*, 4203.
(20) Fujino, T.; Arzhantsev, S. Y.; Tahara, T. *J. Phys. Chem. A* **2001**, *105*, 8123.
(21) Cattaneo, P.; Persico, M. *Phys. Chem. Chem. Phys.* **1999**, *1*, 4739.
(22) Ishikawa, T.; Noro, T. *J. Chem. Phys.* **2001**, *115*, 7503.
(23) Quenneville, Ph.D. Thesis, University of Illinois, Urbana, IL, 2003.
(24) Tiago, M. L.; Ismail-Beigi, S.; Louie, S. *J. Chem. Phys.* **2005**, *122*, 094311.
(25) Ciminelli, C.; Granucci, G. ; Persico, M. *Chem.—Eur. J.* **2004**, *10*. 2327.
(26) Cembran, A.; Bernardi, F.; Garavelli, L.; Gagliardi, L.; Orlandi, G. *J. Am. Chem. Soc.* **2004**, *126*, 3234.
(27) Gagliardi, L.; Orlandi, G.; Bernardi, F.; Cembran, A.; Garavelli, M. *Theor. Chem. Acc.* **2004**, *111*, 363.
(28) Diau, E. W.-G. *J. Phys. Chem. A* **2004**, *108*, 950−956.
(29) Chang, C.-W.; Lu, Y.-C.; Wang, T.-T.; Diau, E. W.-G. *J. Am. Chem. Soc.* **2004**, *126*, 10109.
(30) Blevins, A. A.; Blanchard, G. J. *J. Phys. Chem.* **2004**, *108*, 4962.
(31) Frisch, M. J.; Trucks, G. W.; Schlegel, H. B.; Scuseria, G. E.; Robb, M. A.; Cheeseman, J. R.; Montgomery, J. A., Jr.; Vreven, T.; Kudin, K. N.; Burant, J. C.; Millam, J. M.; Iyengar, S. S.; Tomasi, J.; Barone, V.; Mennucci, B.; Cossi, M.; Scalmani, G.; Rega, N.; Petersson, G. A.; Nakatsuji, H.; Hada, M.; Ehara, M.; Toyota, K.; Fukuda, R.; Hasegawa, J.; Ishida, M.; Nakajima, T.; Honda, Y.; Kitao, O.; Nakai, H.; Klene, M.; Li, X.; Knox, J. E.; Hratchian, H. P.; Cross, J. B.; Bakken, V.; Adamo, C.; Jaramillo, J.; Gomperts, R.; Stratmann, R. E.; Yazyev, O.; Austin, A. J.; Cammi, R.; Pomelli, C.; Ochterski, J. W.; Ayala, P. Y.; Morokuma, K.; Voth, G. A.; Salvador, P.; Dannenberg, J. J.; Zakrzewski, V. G.; Dapprich, S.; Daniels, A. D.; Strain, M. C.; Farkas, O.; Malick, D. K.; Rabuck, A. D.; Raghavachari, K.; Foresman, J. B.; Ortiz, J. V.; Cui, Q.; Baboul, A. G.; Clifford, S.; Cioslowski, J.; Stefanov, B. B.; Liu, G.; Liashenko, A.; Piskorz, P.; Komaromi, I.; Martin, R. L.; Fox, D. J.; Keith, T.; Al-Laham, M. A.; Peng, C. Y.; Nanayakkara, A.; Challacombe, M.; Gill, P. M. W.;

Johnson, B.; Chen, W.; Wong, M. W.; Gonzalez, C.; Pople, J. A. *Gaussian 03*, revision C.02; Gaussian, Inc.: Wallingford, CT, 2004.
(32) Becke, A. D. *J. Chem. Phys.* **1993**, *98*, 5648.
(33) Hariharan, P. C.; Pople, J. A. *Theor. Chim. Acta* **1973**, *28*, 213.
(34) Biswas, N.; Umpathy, S. *J. Phys. Chem. A* **1997**, *101*, 5555.
(35) Traettenberg, M.; Hilmo, I.; Hagen, K. *J. Mol. Struct.* **1977**, *39*, 231.
(36) Bouwstra, J. A.; Schouten, A.; Kroon, J. *Acta Crystallogr., Sect. C* **1983**, *39*, 1121.
(37) Mostad, A.; Romming, C. *Acta Chem. Scand.* **1971**, *25*, 3561.
(38) Fliegl, H.; Kohn, A.; Hattig, C; Ahlrichs, R. *J. Am. Chem. Soc.* **2003**, *125*, 9821.
(39) Anderson, J. A.; Petterson, R.; Tegner, L. *J. Photochem.* **1982**, *20*, 17.
(40) Nagele, T.; Hoche, R.; Zinth, W.; Wachteil, J. *Chem. Phys. Lett.* **1998**, *272*, 48.
(41) Tully, J. C. *J. Chem. Phys.* **1990**, *93*, 1061.
(42) Kasha, M. *Discuss. Faraday Soc.* **1950**, *9*, 14.
(43) Fujino, T.; Arzhantsev, S. Y.; Tahara, T. *Bull. Chem. Soc. Jpn.* **2002**, *75*, 1031.
(44) Kikuchi, O.; Azuki, M.; Inadomi, Y.; Moriais, K. *J. Mol. Struct.* **1999**, *468*, 95.
(45) Hirose, Y.; Yui, H.; Sawada, T. *J. Phys. Chem. A* **2002**, *106*, 3067.